AN ABSTRACT OF THE THESIS OF

David Ly for the degree of Master of Science in Genetics presented on March 30, 2009.
Title: Investigation of *Cis*-acting RNA Element Role in Bovine Viral Diarrhea Virus Replication

Abstract approved:

Ling Jin

Bovine viral diarrhea virus (BVDV) is an enveloped, single-stranded positive-sense RNA virus. The BVDV genome is about 12.5 kb long and consists of a single open reading frame (ORF) flanked by untranslated regions at the 5' and 3' ends (5'-UTR and 3'-UTR, respectively). To investigate the role of *cis*-sequences of UTRs during BVDV replication, we designed four peptide-conjugated phosphorodiamidate morpholino oligomers (PPMO) that are complementary to nucleotides (nt) 10-33 (BVDV-10), 258-281 (BVDV-258), 375-398 (BVDV-375), and 12503-12526 (BVDV-12503) of the BVDV genome. PPMO with sequences targeting nt 258-281 (BVDV-258), 375-398 (BVDV-375), and 12503-12526 (BVDV-12503) of the BVDV genome completely blocked BVDV replication *in vitro*, while the PPMO with sequence complementary to nt 10-33 (BVDV-10) did not have observable inhibition against BVDV virus replication. In addition, BVDV-375 and BVDV-12503 were able to inhibit virus replication at the viral RNA synthesis level. Our study demonstrated that the *cis*-sequences nt 258-281 and 375-398 in the 5'-UTR and nt 12503-12526 in the 3'-UTR are important for BVDV replication, while the *cis*-sequence nt 10-33 may not play a significant role during virus replication.

Investigation of *Cis*-acting RNA Element Role in Bovine Viral Diarrhea Virus Replication

by

David Ly

A THESIS

submitted to

Oregon State University

in partial fulfillment of
the requirements for the
degree of

Master of Science

Presented March 30, 2009
Commencement June 2009

Master of Science thesis of David Ly
presented on March 30, 2009

APPROVED:

Major Professor, representing Genetics

Director of the Genetics Program

Dean of the Graduate School

I understand that my thesis will become part of the permanent collection of Oregon State University libraries. My signature below authorizes release of my thesis to any reader upon request.

David Ly, Author

ACKNOWLEDGEMENTS

I would first like to thank everyone in Dr. Jin's lab. This includes Dr. Jin for providing me with this opportunity to gain valuable research experience and especially for financially supporting me my first year of graduate school, despite being low on funding at the time. In addition, I thank her for exposing me to the research field and what it is all about, considering I did not have any idea when I was at my undergraduate institution. I would also like to thank Megan Moerdyk-Schauwecker, who was the former laboratory technician in our lab. Though she is not with us anymore, I would like to take this opportunity to thank her for instructing someone like me who came into the lab with little research experience but was willing to give it his all if given the opportunity. Finally, I want to thank Kathleen Eide, a graduate student in the MCB program who is also in my lab. She has helped me on my project on numerous occasions, and I enjoy learning new things from her many years of experience working in the lab setting.

Next, I would like to thank Dr. Hiro Nonogaki from the horticulture department. He is truly inspirational and a very down-to-earth guy, and after hearing from his wife about his story to pursue a PhD, I can confidently say that he is one of the few that has achieved the American dream. Also, I would like to thank my other committee members, Dr. Theo Dreher, Dr. Michael Freitag, and Dr. Donna Champeau. I enjoy their company on both professional and personal levels and the fact that they view me as an individual and not just another graduate student, which is one of the main reasons why they are on my committee.

I would also like to take the time to thank people from my undergraduate institution, Linfield College. First, I would like to thank my academic advisor during my undergra-

duate years, Dr. Michael Roberts. He is like a grandfather figure to me and is one of the reasons why I enjoyed life at Linfield. His professional attitude and interest in getting to know other students and myself on a personal level is something I truly admire. Also, I would like to thank Dr. Anne Kruchten. Though it was her first year teaching the microbiology course that I took during my senior year which led to my interest in microbiology, I was impressed with her excellent instruction ability. Her enthusiasm and wit is something that will definitely benefit the college, and though she ended up third in seniority in the department after being there for just one year, I can safely say that the biology department is in good hands with the younger generation of professors. Finally, I really would like to thank Michele Tomseth from the International Programs Office. Her advice on how to survive graduate school was what kept me going and is one of the reasons why I am still here today. I really enjoy her sense of humor and am touched with her interest in my uneventful life, and thus I promise that the next time I visit Linfield the two of us will definitely have lunch together.

Finally, on a personal note, I would like to thank my good friend, Shigeji. A lot of things have occurred to both of us since last year, but I do believe that things will turn out for the better at the end. I do not know if our paths will ever cross again or if we will get a chance to meet each other ever again, but I truly want to say thank you. I wish him the best of luck with whatever he chooses to pursue in life, and even though he will be returning to Japan soon, I hope he knows that I will always be supporting him in the U.S. while optimistically anticipating that our paths will cross someday.

TABLE OF CONTENTS

TABLE OF CONTENTS (continued)

LIST OF FIGURES

LIST OF TABLES

Investigation of *Cis*-acting RNA Element Role in Bovine Viral Diarrhea Virus Replication

1. Introduction

1.1 Bovine Viral Diarrhea Virus: General

Bovine viral diarrhea virus (BVDV) is a member of the *Pestivirus* genus of the *Flaviviridae* (Pankraz et al., 2005). BVDV is an enveloped, single-stranded, positive-sense RNA virus. The genome size of BVDV is approximately 12.5 kilobases in length, but this can vary to as large as 16 kb depending on the biotypes, either cytopathic (CPE) or non-cytopathic (non-CPE) (Zhang et al., 1996). The BVDV genome consists of a single, long open reading frame (ORF) flanked by a 5'-untranslated region (UTR) of about 385 nucleotides and a 3'-UTR of about 220 nucleotides (Gong et al., 1996). Pestivirus genome RNAs lack a 5' cap structure, and do not terminate with a poly(A) tail but rather with a poly(C) tract (Rice, 1996). After translation of the ORF, the single protein of about 4000 amino acids is subjected to processing and cleaving by cellular and viral-encoded proteases to give rise to the structural and non-structural proteins required in BVDV replication (Zhang et al., 1996).

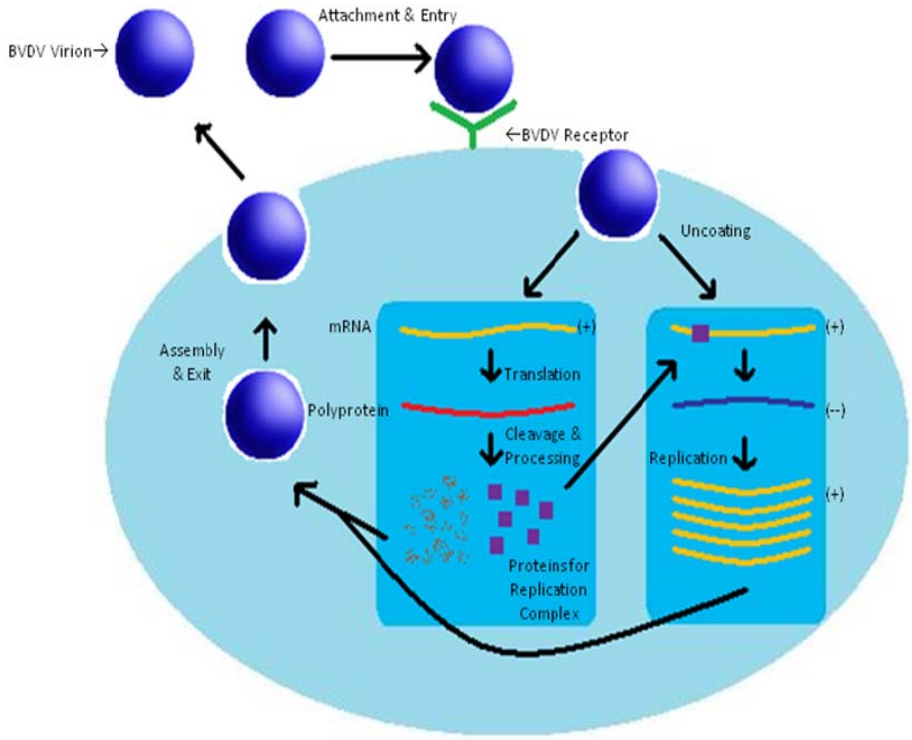

Figure 1. The replication lifecycle of BVDV.

Virus Replication

The entry of BVDV into target cells begins with attachment. The attachment is mediated mainly by binding of BVDV envelope glycoproteins E2 (Thiel et al., 1996) to host cell receptors, which have yet to be identified. The entry is via receptor-mediated endocytosis (Gong et al., 1996). Following endocytosis, the viral nucleic acid is released into the cytoplasm. Though the early events of BVDV replication are not fully understood, it is known that the genome of positive-sense RNA viruses can be readily translated into a polyprotein. Multiple AUG codons are found in the 5'-UTR of the BVDV genome, but

the authentic AUG codon at nt 386-388 is believed to be involved with translation initiation (Deng and Brock, 1993). Within the 5'-UTR are *cis*-acting RNA elements that make up the internal ribosome entry site (IRES), which serves to initiate protein translation by recruiting ribosomes. Whereas eukaryotic mRNA transcripts are capped at the 5' end and are required to be capped for recruiting eukaryotic initiation factors, the absence of cap structures in BVDV and other pestiviruses means that a cap-independent mechanism for translation is necessary. The role of *cis*-acting RNA elements within the 5'- and 3'-UTR will be explored in this study.

BVDV RNA replication is similar to other positive-sense RNA viruses, such as poliovirus. The viral genome replication starts out with the positive-sense RNA being copied into negative-sense RNA, serving as a template for the synthesis of more positive-sense RNA. This process requires viral RNA-dependent RNA polymerase, a helicase, host cellular proteins, and viral cofactors (Gong et al., 1996). Replication occurs asymmetrically in the host cell's cytoplasm, which means that over time increasing amounts of positive-sense RNA molecules are produced in comparison to negative-sense RNA (Yu et al., 1999).

The BVDV viral genome encodes structural proteins (C, E0, E1, E2) and non-structural proteins (N^{pro}, NS2, NS3, NS4A, NS4B, NS5A, NS5B). The C protein is the nucleocapsid protein that makes up the capsid of the virion. The C protein has a basic RNA-binding domain located at the N-terminal region of the polyprotein and functions to encapsidate and coat the viral RNA (Ivanyi-Nagy et al., 2008). E0, E1, and E2 are envelope-associated glycoproteins. E2 is the surface glycoprotein that aids in attachment

to receptors on target cells. Though the type of interaction between E0 and the virion is unclear, E1 and E2 are the major antigens of BVDV. The variation of amino acid sequences in E2 is used to distinguish variation among pestiviruses and different BVDV strains, such as NADL, SD-1, and Osloss (Thiel et al., 1996). Based on the major antigen of the virus, BVDV is classified into two main genotypes, BVDV-1 and BVDV-2 (Fulton et al., 2005).

Nonstructural proteins function mainly in viral RNA replication. NS23 protein is found in the non-CPE biotype of BVDV and is further processed to NS2 and NS3 in the CPE biotype. NS3 is highly conserved in pestiviruses and is used to distinguish between the two biotypes. NS3 has protease and NTPase activity and is a virulence factor of CPE BVDV (Thiel et al., 1996). The NS5A protein is required for viral RNA replication, but its exact role, along with NS2, NS4A, and NS4B, remains unclear (Pankraz et al., 2005).

The packaging of RNA and assembly of progeny virions is still not well understood, but the exit of assembled virions is believed to occur by budding into an intracellular membrane compartment, such as the endoplasmic reticulum. After being sent through the host secretory pathway, the virion is released at the cell surface and is then able to infect other neighboring cells (Thiel et al., 1996).

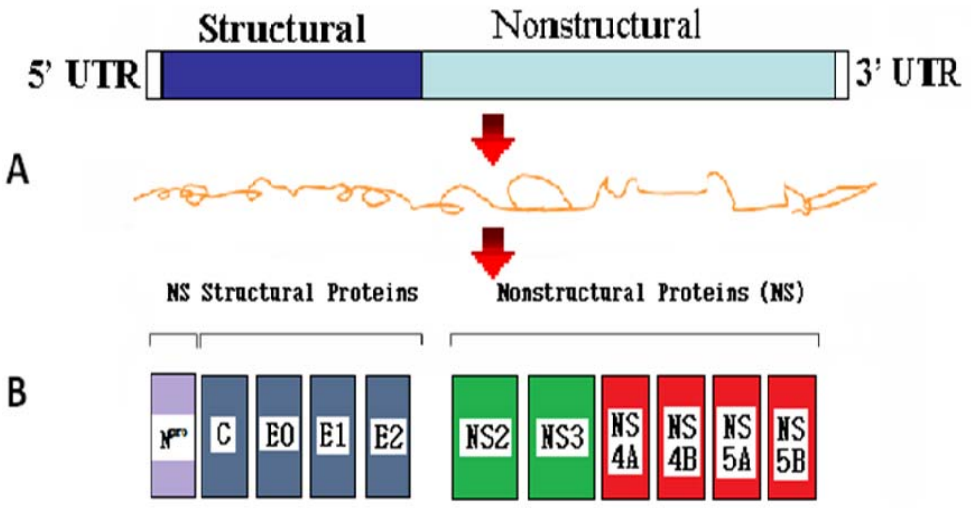

Figure 2. Schematic diagram of the BVDV genome. (A) Translation of the single ORF yields a polyprotein that is further processed and cleaved by proteases to (B) yield the different structural and non-structural proteins needed for virus replication. With the exception of N^{pro}, which is upstream of the structural proteins, nonstructural proteins are located downstream of the structural proteins in BVDV.

1.2 The 5'-UTR & IRES

5'-UTR

The 5'-UTR of BVDV is between 345 and 385 nucleotides long. Computer analyses using the RNA FOLD program show that BVDV 5'-UTRs form a unique secondary structure with four main structural domains labeled I, II, III, and IV (Figure 3), where numbering of the nucleotides starts at the 5' terminal end (Brown et al., 1992). Figure 4 shows an alternative view of the 5'-UTR from another study using both the RNA FOLD and HIBIO DNASIS program that gives a better distinction between the domains. Instead of using I, II, III, and IV to label the four structural domains, letters A through D are used as designations. In addition, because of the large size and the presence of different stem-loop structures in Domain D, the fourth domain is divided into subdomains D1 through D5. For consistency reasons, however, Figure 3 will be used for references to specific domains, nucleotide positions, and regions at the 5'-UTR since the boundaries where each domain starts and ends is different between the two predicted 5'-UTR structures.

Approximately 70% of the nucleotides contribute to the overall secondary structure by base-pairing. Most of the 5'-UTR nucleotide sequence is conserved in different strains of BVDV (NADL, SD-1, and Osloss). However, there are three variable regions in the 5'-UTR. The first variable region extends from nucleotides 1-72, the second one stretches from nucleotides 206-221, and the third one covers nucleotides 280-320 (Deng and Brock, 1993). The left portion of Domain I (nucleotides 1-68) is conserved between BVDV strains NADL, SD-1, and Osloss (Brown et al., 1992). The right loop of Domain

I is located in the first variable region and does not seem to be conserved among pestiviruses. Domain II (nucleotides 69-138) contains a single loop structure, and although it is conserved in the pestiviruses, a small portion of nucleotides at the 5' end are located in the first variable region. Domain III starts at nucleotide 139 and ends at nucleotide 361, comprising of about two-thirds of the 5'-UTR. This large domain also contains the second and third variable regions of the primary sequence. Domain IV starts at nucleotide 362 and ends after the AUG start codon (Deng and Brock, 1993).

Besides the AUG start codon in Domain IV, multiple cryptic AUG codons are found in 5'-UTRs of pestiviruses. The number of AUGs in the different pestiviruses range from 5 to 8. Two of these start codons, nucleotides 108-110 and 379-381, are conserved in all five pestiviruses. The authentic AUG in pestiviruses actually has a weak context for initiation, in which an adenine or guanine would be more favorable than the cytosine at position -3. Two of the cryptic start codons, nucleotides 131-133 in BVDV NADL and SD-1 and 312-314 in two hog cholera virus (HoCV) strains, a close relative of BVDV in the *Pestivirus* genus, are strong initiation codons that allow efficient translation initiation (Deng and Brock, 1993). Although not a topic of research in this study, examining these cryptic start codons would provide some additional insight on components essential for translation initiation.

In addition to studies done by Deng and Brock, 1993, later studies using phylogenetic, biochemical probing, and mutational analyses have also examined the secondary structure of pestivirus 5'-UTRs. There have not been many revisions to the secondary structure of pestivirus 5'-UTRs in general; pestivirus 5'-UTRs contain a hairpin loop structure

at the 5’ terminal end of Domain I, Domain II comprises of a large stem-loop structure, many internal stem-loops are found within Domain III, and a pseudoknot structure forms at the 3’ end (Rijnbrand et al., 2004). One difference that is present, however, is the lack of a fourth structural domain in some recent publications, where Domain III and Domain IV are combined as one large domain (Grassmann et al., 2005).

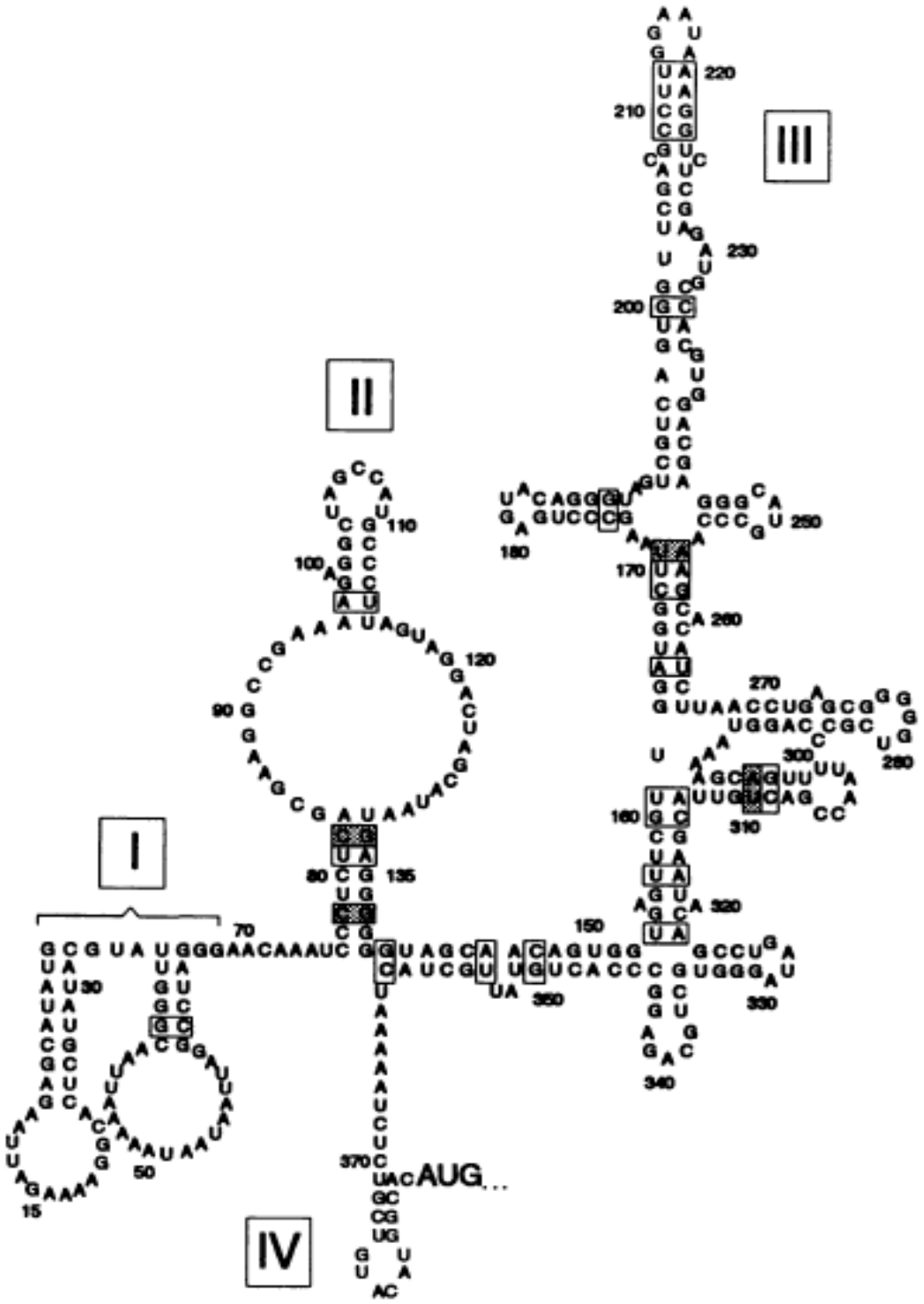

Figure 3. Secondary structure of the 5'-UTR of the BVDV genome (NADL strain). The four major structural domains are labeled I through IV, and numbering of nucleotides starts at the 5' terminal end. Nucleotides in shaded boxes represent sites of covariation

between NADL and Osloss strains, and nucleotides in open boxes are sites of covariant substitutions between different BVDV and HCoV strains (from Brown et al., 1992).

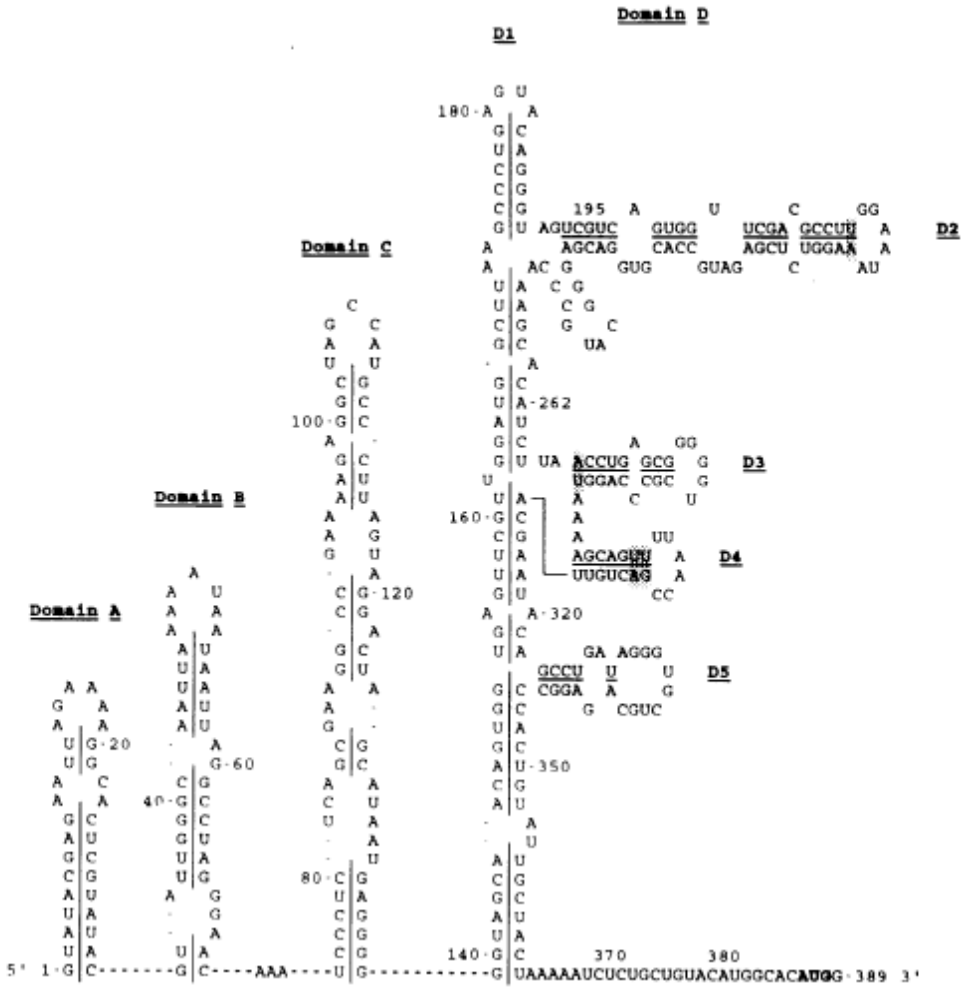

Figure 4. Alternative view of the 5'-UTR of the BVDV genome (NADL strain). The four major structural domains are labeled Domain A through D, while Domain D is divided into subdomains D1 through D5. Numbering of nucleotides starts at the 5' terminal end (from Deng and Brock, 1993).

BVDV Internal Ribosome Entry Site (IRES)

IRESes in the 5'-UTR can initiate translation of the ORF independent of a 5' cap structure. IRES sequences are used by many RNA viruses for translation initiation. This is achieved by recruitment of ribosomal complexes to the initiation codon, and because this recruitment is direct, eukaryotic cap-binding complexes such as eIF4F are not needed (Kolupaeva et al., 2000). Requirements for IRES activity differ depending on the virus. The first step of translation initiation in Hepatitis C Virus (HCV), for example, requires the 40S ribosomal subunit to interact with the RNA to assemble 48S initiation complexes. Nonetheless, according to studies done on IRESes of different viruses, the efficiency of IRES activity depends mainly on RNA folding (Martínez-Salas et al., 2008).

Many positive-sense RNA viruses have numerous structural motifs in the UTRs. Regardless of whether or not they are part of an IRES, these elements have important roles in the life cycle of the virus. Because of these unique motifs that serve as important structural domains, they are recognized and bound by host and viral proteins responsible for viral RNA replication and/or translation. These proteins are suggested to function as mediators between the UTRs, serving as signals that allow the 5'- and 3'-UTR to "communicate" with each other (Martínez-Salas et al., 2008). A study conducted with the 5'- and 3'-UTR of hepaciviruses, for example, demonstrated the presence of replication signals where host factors called NFAR proteins would bind to specific RNA-binding motifs on the ends of the HCV genome (Isken et al., 2007).

Viral IRESes are different between distantly related virus families, while closely related viruses share conserved RNA structures. Features of pestivirus 5'-UTRs are more

similar to picornaviruses and HCV than to other members of the Flaviviridae family (Martínez-Salas et al., 2008). Studies with HCV demonstrate that there are differences between HCV 5'-UTRs and pestivirus UTRs. For example, Domain II and the hairpin loop in Domain I is longer in length in HCV, and there are fewer internal stem-loops in HCV than in pestiviruses. Other than these minor differences, the overall structures of both groups share a high degree of similarity (Fletcher and Jackson, 2002). On the other hand, the functions of particular regions have distinct differences. In HCV, the IRES is suggested to be in Domain II and III where overlapping replication and translation signals are found. Mutagenesis experiments showed that Domain I actually downregulates IRES activity, whereas BVDV experiments showed that the terminal hairpin at the 5' end serves as a bifunctional motif with roles in both gene expression and viral RNA synthesis (Grassmann et al., 2005).

A unique feature of pestivirus IRESes is that they extend into the coding region, which is not the case in picornavirus IRESes. Even though ongoing research on the BVDV IRES is still being conducted, it is suggested that the IRES starts somewhere in the second domain of the 5'-UTR and extends into the ORF itself (Moes and Wirth, 2007). Early experiments that involved deletion of the coding region showed reduction of IRES activity; however, the exact location of how far the BVDV IRES extends has not been investigated in great detail (Fletcher and Jackson, 2002). Computational analysis in the SD-1 strain of BVDV suggests the BVDV IRES is 330-380 nucleotides in length and that a pseudoknot structure is important for IRES function, where this pseudoknot structure is predicted to be between the end of Domain III and the AUG start codon. Also,

while 80% of the 5'-UTR consists of the IRES, the other 20% is predicted to be in Domain I and not essential for translation (Moes and Wirth, 2007). However, there is ongoing controversy in terms of where the 5' boundary of the pestivirus IRES, including the BVDV IRES, lies. Early experiments using bicistronic reporter constructs showed that Domain I is dispensable for protein translation and that the 5' boundary of the BVDV IRES starts around nt 75 (Chon et al., 1998). These results agree with a later study done on HoCV, a close pestivirus relative of BVDV, where the authors also showed that Domain I is not essential for IRES function (Fletcher and Jackson, 2002). On the other hand, later mutagenesis experiments showed that Domain I of the BVDV 5'-UTR not only optimizes IRES activity, the region between the terminal hairpin and Domain II is suggested to serve a secondary structure maintenance function to preserve the hairpin (Grassmann et al., 2005). Thus, some minor controversy about the importance of the terminal hairpin and the exact boundaries of the BVDV IRES still exists and is an ongoing research topic.

1.3 The 3'-UTR

Pestivirus 3'-UTRs consist of both variable and conserved regions. The variable region starts at the polyprotein stop codon and spans more than 120 nucleotides, ending near the top of the second stem-loop structure (Figure 5). The conserved region of about 100 nucleotides starts immediately after the end of the variable region and stretches to the 3' terminal end (Isken et al., 2004). An example of a major difference in the variable region between pestivirus strains is a 41 base deletion in the Osloss strain of BVDV, which explains the smaller 3'-UTR in BVDV Osloss compared to other pestiviruses. The variation suggests that this short nucleotide sequence is not essential but serves a secondary maintenance role for essential regions (Deng and Brock, 1993).

Secondary structure of the 3'-UTR in pestiviruses is similar between different BVDV strains. Analyses using the HIBIO DNASIS computer program show that the 3'-UTR of BVDV contains three stem-loop structures separated by single-stranded RNA regions (Pankraz et al., 2005). However, using the RNA FOLD program a different secondary structure of the 3'-UTR in pestiviruses was predicted, with each domain labeled SL I, SL II, SL III, and SL IV (see Figure 5). The main difference between the two models is the number of stem-loop structures found beyond SL II, which is not investigated in this study.

An RNA structural motif found in the 3' terminal end of the 3'-UTR is a stem-loop structure designated SL I. This stable stem-loop is located in the conserved region that has a string of five C residues located at the 3' terminal end. The next stem-loop structure is SL II, which has a significantly lower thermodynamic stability than that of SL I

and is located in both the conserved and variable region (Yu et al., 1999). Between the two stem-loops is a stretch of nucleotides (ACAGCACUUUA) that is conserved in five BVDV strains (see Figure 5). This highly conserved sequence between SL I and SL II, denoted SS, along with SL I at the 3'-terminus may have critical functions in virus replication. Evidence includes studies of mutant RNAs with mutations in different parts of the 3'-UTR. RNAs with mutations in the five C residue nucleotide stretch located at the 3' terminal end affect virus infection (Yu et al., 1999). Mutants with deletions in SS inhibited virus replication, while deletions in the upstream part of the 3'-UTR had only minor replication inhibition effects. Mutant RNAs containing whole deletions of SL I that was then transfected into host cells completely blocked virus replication, suggesting that SL I is required for BVDV replication (Pankraz et al., 2005).

Other studies have proposed that the C residue stretch at the 3' end, SL I, and SS comprise of an RNA element that functions as a negative-sense RNA synthesis promoter for initiation of negative-sense RNA synthesis. These RNA structural motifs initiate synthesis of negative-sense RNA by direct assembly of the replication initiation complex (Yu et al., 1999). An example of 3'-UTR contribution to RNA synthesis was reported in flaviviruses. Interaction between ribosomal complexes and the 3'-UTR facilitated 3'-UTR and replication complex association, leading to negative-sense RNA synthesis (Martínez-Salas et al., 2008). Besides replication complexes, *trans*-acting host factors are also believed to be involved in the synthesis process, which will be described in more detail later in this section.

SL III and SL IV, or SL_{stop}, are part of the variable region (Deng and Brock, 1993). The two stem-loops along with SL II are unstable structures. Mutant viruses with deleted SL III showed no difference of infectivity compared to wild-type BVDV. Viral RNA with deletion of the entire SL II did not show significant reduction of virus titer, implying that SL II is dispensable (Pankraz et al., 2005). However, a study using BVDV replicons demonstrated that both SL II and SL III are required structures for proper translation termination (Isken et al., 2004). Thus, there is still minor controversy and ongoing research on the importance of SL III and IV.

One function of the variable region of the 3'-UTR is to directly assemble replication complexes. This is believed to be accomplished through recruiting the NFAR host factors that bind both the 5'- and 3'-UTR and has direct roles in virus replication, possibly by stabilizing the secondary structure of the variable region to induce its function (Isken et al., 2004). Evidence includes reports of the proteins binding to both SL II and SL III in a BVDV replicon during RNA replication (Pankraz et al., 2005). In addition, interactions of the 3'-UTR with viral proteins NS3 and NS5B, which are the protease and RNA-dependent RNA polymerase, respectively, have been reported to be described with Japanese encephalitis virus and dengue virus (Yu et al., 1999). Thus, not only are there *cis*-acting RNA elements to aid with virus replication, but *trans*-acting host and viral proteins associate with the UTRs to mediate activity of the RNA elements.

Another role of the 3'-UTR is regulating the termination of translation. There must be a balance between RNA synthesis and protein translation to ensure efficient viral propagation. RNA synthesis and protein translation, in principle, cannot occur at the

same time. While ribosomes are moving along the viral RNA in the 5' to 3' direction, the RNA-dependent RNA polymerase moves along the RNA in the 3' to 5' direction to synthesize negative-sense RNA. Thus, both processes would need to occur consecutively, not simultaneously, to prevent interference of the replication and translation machinery with each other (Gamarnik and Andino, 1998).

The conserved region is involved in controlling assembly of the replication complex, whereas the variable region is responsible for switching between RNA synthesis and protein translation. The order of events would begin with RNA-RNA interactions or the binding of NFAR proteins that allow contact between the two UTRs. Then, with translation initiation signals located in the 5'-UTR, the 3'-UTR variable region cooperates in initiating translation, which may include a conformational change in RNA. In the initiation of RNA synthesis, the replication complex is assembled at the conserved region of the 3'-UTR, and the variable region is responsible for suppressing translation initiation. This can happen via the replication complex changing the conformation of the variable region so that the 5'-UTR is affected and causing translation to cease. Ribosomes would then fail to associate with the viral RNA, allowing RNA replication to occur (Isken et al., 2003).

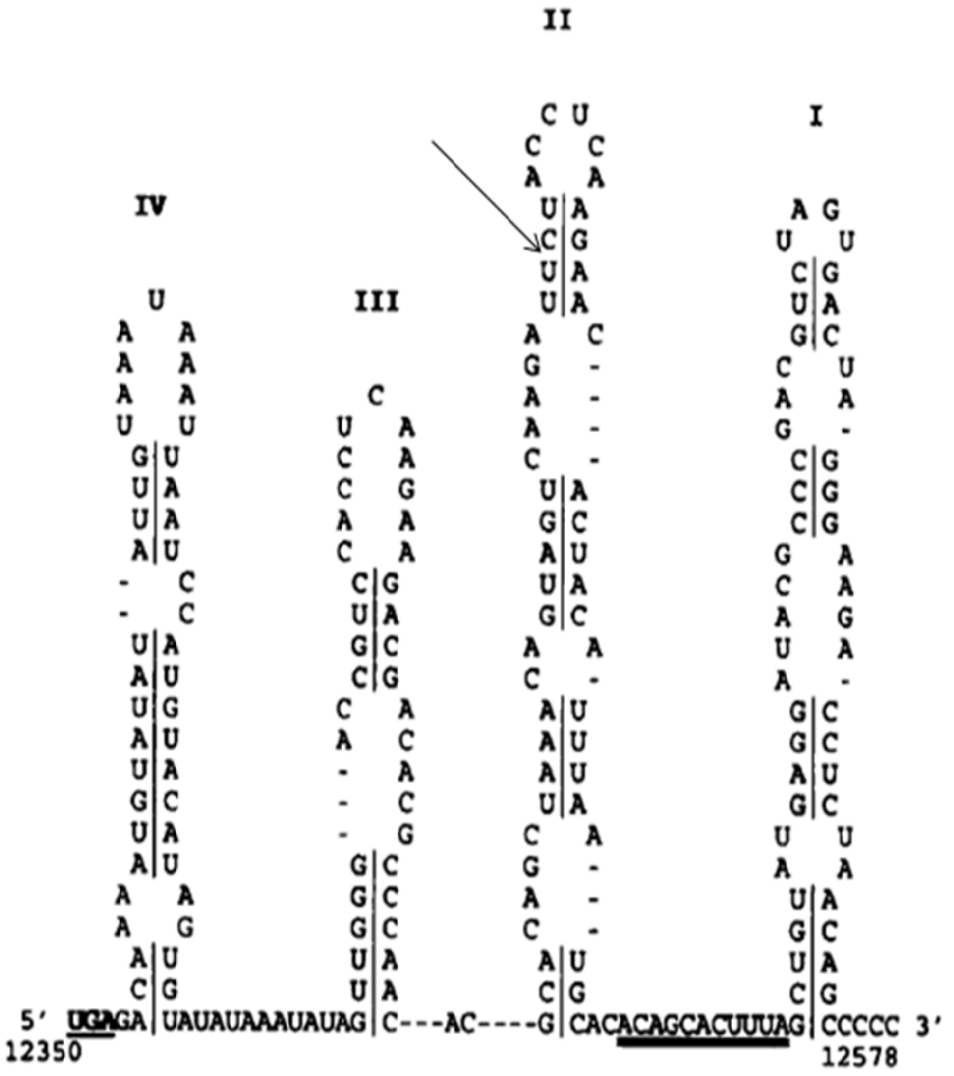

Figure 5. Secondary structure of the 3'-UTR of the BVDV genome (NADL strain). The four stem-loop structures are designated as stem-loop (SL) I through IV in the 3' to 5' direction. Both the polyprotein stop codon UGA (lower left) and the conserved linear sequence between SL I and SL II (lower right) are underlined. The arrow marks the border between the variable and conserved regions located at the 5' and 3' side, respectively (from Deng and Brock, 1993).

1.4 Phosphorodiamidate Morpholino Oligomers

Phosphorodiamidate morpholino oligomers (PMO) are single-stranded nucleic acid oligomers with a modified backbone composed of nitrogen-containing morpholine rings joined by phosphorodiamidate intersubunit linkages. The analogues are water soluble, resistant to cellular nucleases, and typically synthesized to a length of 18-25 bases (Deas et al., 2005). PMO can hybridize to a complementary sequence in target mRNA and can reduce mRNA translation through steric blocking (Yuan et al., 2006). Conjugation of an arginine-rich cell-penetrating peptide (CPP) to the 5' end of a PMO, creating a peptide-conjugated PMO (PPMO), has been shown to enhance uptake into cells (Patel et al., 2008). PPMO have been shown to inhibit infections by a number of RNA viruses in a sequence-specific and dose-dependent manner in both cell cultures and mouse models (Zhang et al., 2007). In eukaryotes, the mRNA is transcribed in the nucleus. After introns are spliced out of the transcript in the nucleus, it is then transported to the cytoplasm with the help of different transport complexes. Translation initiates when the 40S subunit of the ribosome binds to the mature mRNA along with other eukaryotic initiation factors. This forms the pre-initiation complex which scans the mRNA molecule until it reaches a start codon located in a strong initiation context. The 60S subunit can then attach to the small subunit and allow elongation to occur. Upon binding of the PPMO to its target sequence, the PPMO can physically block the RNA translation initiation complex reaching the start codon and prevent RNA translation, which will consequently inhibit virus replication. An example of PPMO use demonstrated in the literature is inhibiting replication of influenza A virus (FLUAV) (Ge et al., 2006). Other virus studies involving

PPMO use also include West Nile Virus (WNV), Foot and Mouth Disease Virus (FMDV), and Dengue Fever Virus.

The main goal of this research was to investigate roles of viral RNA *cis*-sequences at both the 5'- and 3'-UTR in virus replication and viral RNA replication. In order to study the role of those viral RNAs at the UTRs, we designed PPMO that are complementary to BVDV RNA sequences. PPMO binding to complementary RNA will prevent targeted viral RNA from interaction with host factors and interfere with its function.

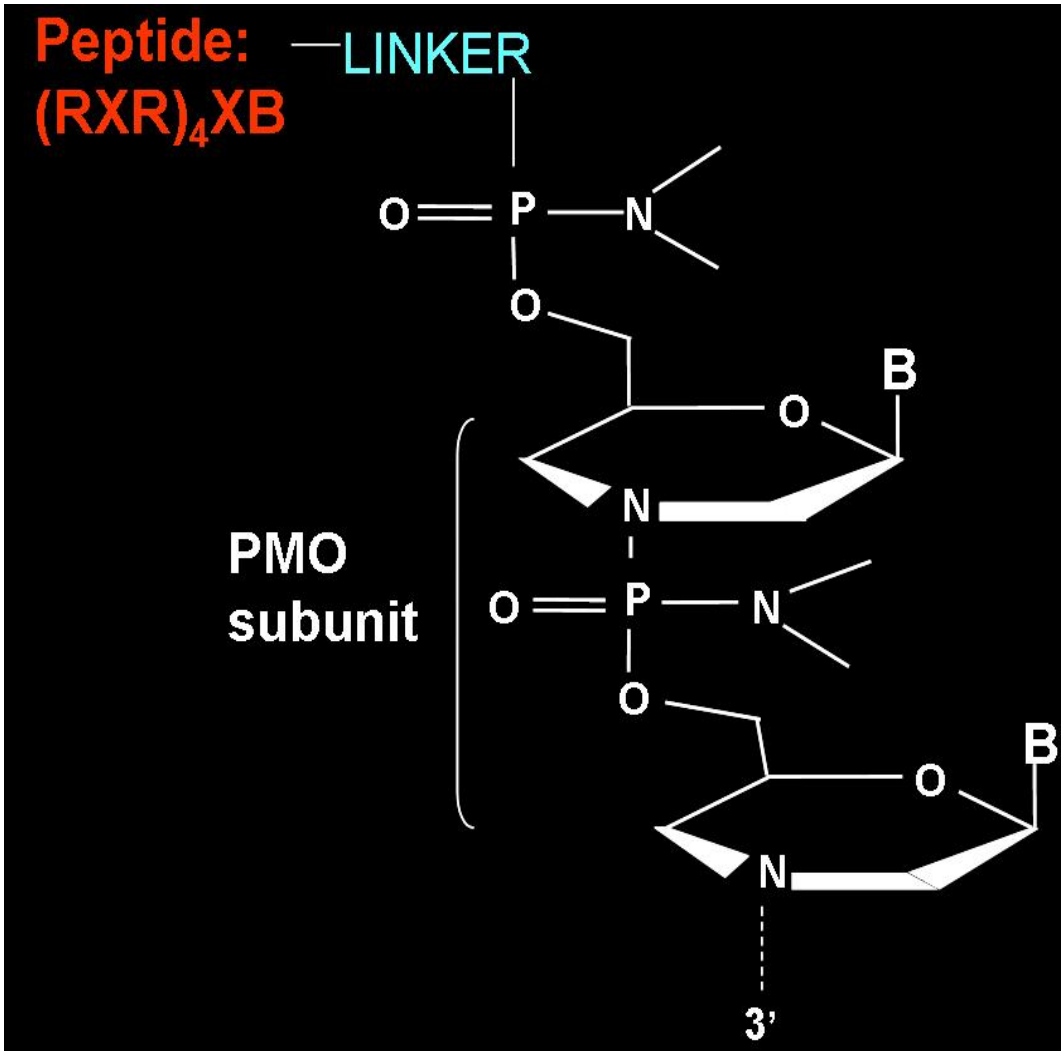

Figure 6. The structure of PPMO, where R=arginine, X=6-aminohexanoic acid, B=β-alanine. The deoxyribose rings and phosphodiester linkages in DNA are replaced by morpholino rings and phosphorodiamidate linkages, respectively. An arginine-rich peptide is covalently conjugated to the 5' end of the PMO through a noncleavable linker to allow the efficient delivery of the compound into target cells.

1.5 Hypothesis

The hypothesis for this research is that sequences nt 10-33 (BVDV-10), 258-281 (BVDV-258), 375-398 (BVDV-375), and 12503-12526 (BVDV-12503) within the BVDV genome (NADL strain) are important for viral RNA synthesis and virus replication, and that the binding of PPMO to those sequences at the 5'- and 3'-UTR will block replication.

The first PPMO that we created was BVDV-10, which is specific for the left portion of Domain I of the 5'-UTR of the BVDV genome. The nucleotide sequence in the apical loop targeted by BVDV-10 is variable among different pestiviruses, and because the BVDV IRES is proposed to start somewhere in Domain II and extend into the ORF, the region which BVDV-10 binds may not be essential for virus replication. However, a review by Martínez-Salas et al., 2008 mentioned that the signals for RNA replication are restricted to Domain I. Thus, this PPMO will provide insight on whether Domain I has important roles in virus replication. Our second PPMO was BVDV-258, which targets part of a stem-loop structure in Domain III of the 5'-UTR. Even though Domain III contains the second and third variable region mentioned earlier, this targeted *cis*-sequence is mostly a conserved region among pestiviruses, and thus it will be interesting to see if this region is important for virus replication. The third PPMO we designed to target the 5'-UTR was BVDV-375. This region targets Domain IV and specifically includes the region containing the authentic AUG codon involved with translation initiation. Thus, this PPMO should be able to effectively inhibit virus replication.

The last PPMO we designed, BVDV-12503, targets the single-stranded region, SS, between SL I and SL II of the 3'-UTR of the BVDV genome. We chose this region because of its conserved nature and easy accessibility for the PPMO to bind. This conserved nucleotide sequence, along with SL I and the single-stranded sequence at the 3' terminal end, are *cis*-acting RNA elements of the 3'-UTR with important roles in virus replication. Specifically, these functional elements are suggested to facilitate synthesis of negative-sense RNA.

1.6 Objectives

The first objective was to examine if PPMO specific to the 5'- and 3'-UTR has any effect on virus replication. A growth kinetics curve was examined by standard $TCID_{50}$ titration (Becher et al., 2001). If the PPMO can block BVDV infection at 100% efficiency, then there should be no cytopathic effects observed in cells pre-treated with PPMO as opposed to cells mock-treated with DMEM medium or DSscr, the random sequence PPMO.

A second objective was to examine if PPMO specific to the 5'- and 3'-UTR has any effect on viral RNA synthesis. If the PPMO can block RNA synthesis by binding to the viral RNA and preventing RNA-dependent RNA polymerase from synthesizing more ±RNA, then cells treated with the PPMO will have a lower BVDV RNA copy number compared to control cells that were treated with DMEM medium or DSscr controls. The viral RNA replication was monitored by quantitative real-time RT-PCR and semi-quantitative RT-PCR methods as described in the Materials and Methods.

2. Materials and Methods

Cells and viruses. Bovine tracheal (BT) cell lines were maintained in Dulbecco's modified Eagle's medium (DMEM) supplemented with 10% fetal bovine serum (FBS) from a BVDV-free herd (Invitrogen), penicillin (100 U/mL), streptomycin (100 μg/mL) (Sigma-Aldrich, Inc.) and gentamycin (10 μg/mL) (Invitrogen) at 37°C with 5% CO_2 in a humidified incubator. The NADL strain of CPE BVDV was grown in BT cells in DMEM media supplemented with 5% BVDV-free FBS and antibiotic as above.

Molecular cloning. A portion of the 5'-UTR of the BVDV genome was reverse transcribed and ligated to a pCR4-TOPO vector as recommended by the manufacturers (Invitrogen). The ligated vector was transformed into chemically competent *E. coli* cells TOP10 as recommended by the manufacturers. Correct insert of the BVDV viral genome was confirmed with endonuclease restriction digestion by EcoRI. The purified plasmid was used to generate a standard curve for quantitative real-time RT-PCR analysis.

Primers. The primers specific for the 5'-UTR used in the RT-PCR reactions were BVDVF373 (5'-ATCACCGACCACATGACAGA-3') and BVDVR373 (5'-CAGGGA CTGGGGTATGAGAA-3') (Invitrogen).

PPMO design and synthesis. All PPMO were synthesized at AVI BioPharma Inc. (Corvallis, OR) by methods previously described (Summerton and Weller, 1997). An arginine-rich peptide abbreviated P7, AC-NH-$(RXR)_4$XB-COOH (where R stands for arginine, X stands for 6-aminohexanoic acid, and B stands for β-alanine) was covalently conjugated to the 5' end of each PMO used in this study. P7-PMO compounds of 24 bases in length were designed to target, by traditional Watson-Crick base pairing, *cis*-

acting RNA elements in the 5'- and 3'-UTR of the BVDV genome that may possess important roles in BVDV replication. The P7-PMO sequences, designations, and target sequences are described in Table 1. A 20-mer P7-PMO called "DSscr" containing a random sequence and 50% G/C content was synthesized and used as a negative control for any non-sequence-specific activity. The P7-PMO sequences along with the DSscr control were screened with BLAST (http://www.ncbi.n lm.nih.gov/BLAST/) against primate and bovine DNA sequences to exclude the possibility of any unintentional hybridization events. Prior to drug treatment, all P7-PMO were resuspended with sterile distilled water to a concentration of 2 mM and stored at 4°C.

Table 1. PPMO names, targets, and sequences.

Name of PPMO	Target	PPMO Sequence
BVDV-10	5'-UTR	5' – CGT-ATA-CGA-GTG-CCT-TTT-CTA-ATT – 3'
BVDV-258	5'-UTR	5' – ACC-CCC-GCT-CAG-GTT-AAG-ATG-TGC – 3'
BVDV-375	5'-UTR	5' – TGA-TCA-ACT-CCA-TGT-GCC-ATG-TAC – 3'
BVDV-12503	3'-UTR	5' – CAT-ACA-GCT-AAA-GTG-CTG-TGT-GCA – 3'
DSscr	---	5' – AGT-CTC-GAC-TTG-CTA-CCT-CA – 3'

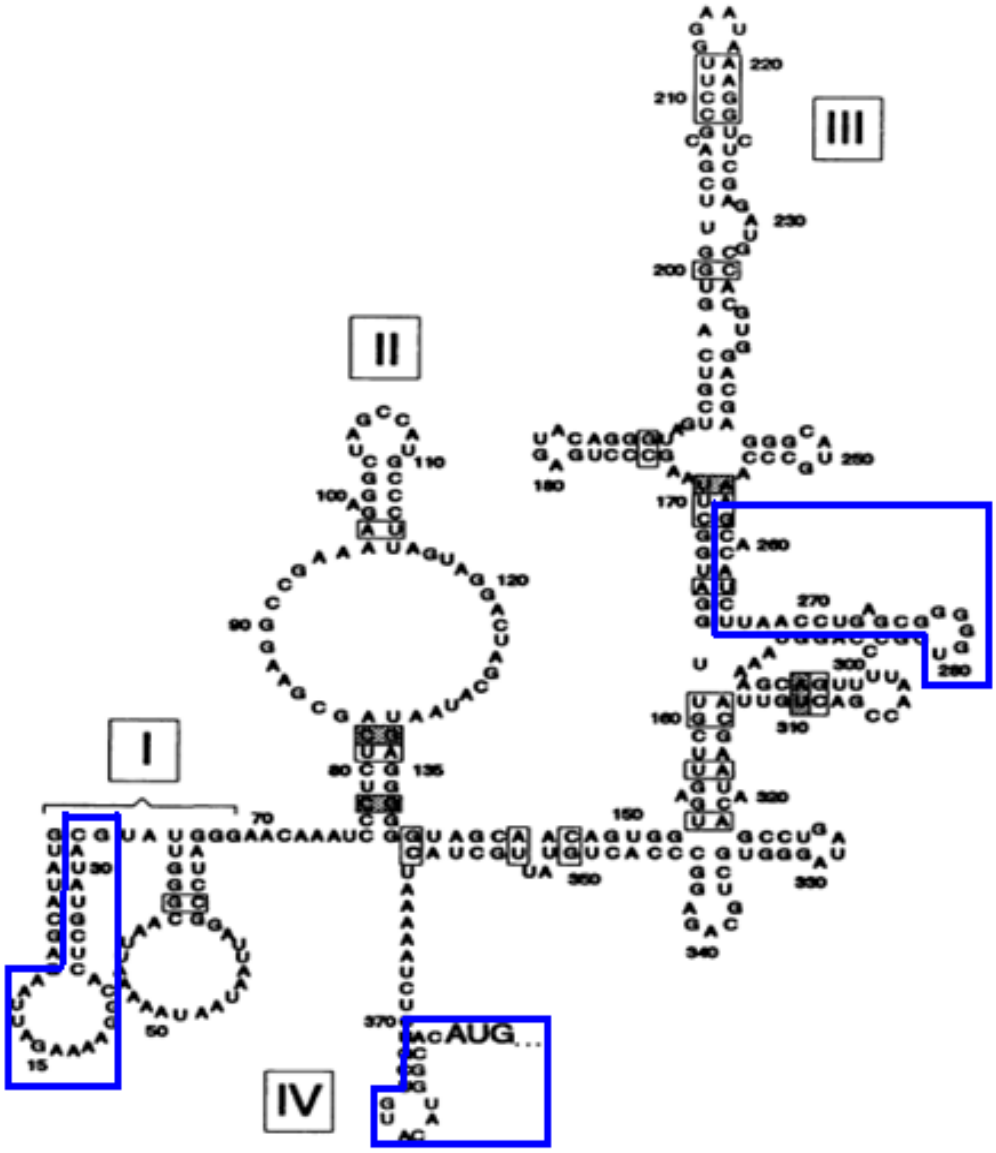

Figure 7. Targeted sequences in the 5'-UTR of the BVDV genome (NADL strain) (from Brown et al., 1992). The boxed regions with blue rectangles are the targeted sequences by PPMO listed in Table 1.

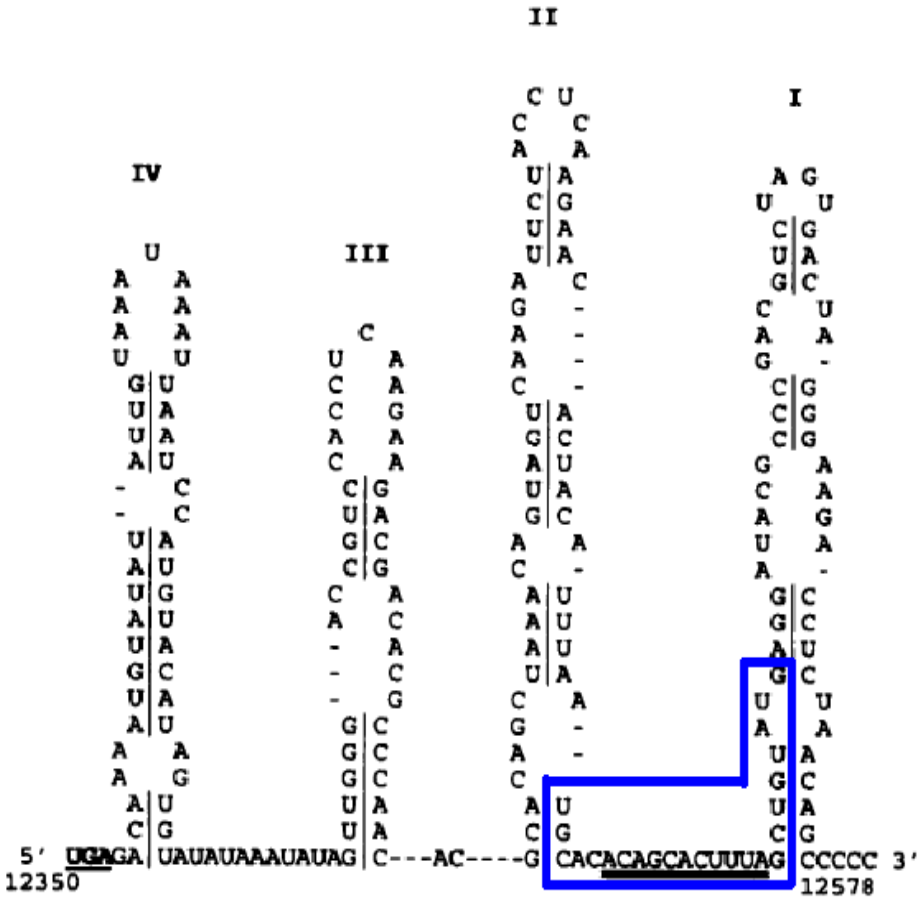

Figure 8. Targeted sequence in the 3'-UTR of the BVDV genome (NADL strain) (from Deng and Brock, 1993). The boxed region in blue is the targeted sequence by PPMO BVDV-12503 as listed in Table 1.

Cell toxicity assay. Twelve-well plates were seeded with 1×10^6 BT cells/well the day before PPMO treatment, washed once with 1× Dulbecco's phosphate-buffered saline (DPBS), and were treated with 0.5 mL of PPMO at 5, 10, 20, 40, 60, and 80 μM, respectively. At 2, 4, and 24 hours post-treatment, the drug was removed and cells were washed twice with 1× DPBS. DMEM medium supplemented with 5% FBS was added, and cell viability was examined using standard microscopy over a period of five days.

Determination of BVDV growth kinetics. Twelve-well plates seeded with 1×10^6 BT cells/well the day before were pre-treated for two hours with plain medium (mock treatment), 20 μM DSscr, or BVDV specific PPMO at 10 μM and 20 μM. Following two hour treatment the plates were washed with PBS, and each well was inoculated with 0.1 mL of 1×10^4 $TCID_{50}$/mL BVDV. The inoculum was removed after the 1 hour absorption, and DMEM medium supplemented with 5% FBS was added. The cell cultures were harvested at 12, 24, and 48 hours post-infection (hpi), and the virus titer was measured by standard $TCID_{50}$/mL titration assay (Becher et al., 2001).

RNA extraction. Total RNA was extracted from BVDV-infected cells and mock-infected cells with TRIzol (Invitrogen). Briefly, 500 μL of TRIzol Reagent was added to each well, and the lysed samples were incubated at room temperature to allow the complete dissociation of nucleoprotein complexes. Chloroform (100 μL) was added before centrifuging the samples at 4°C to separate the mixture into a lower phase (chloroform), an interphase (DNA and protein), and an upper aqueous phase (RNA). The RNA was precipitated by the mixing of isopropyl alcohol (250 μL) with the aqueous phase and then centrifugation to form a clear RNA pellet. After washing with 75% ethanol and vacuum-

drying the RNA product, the pellet was resuspended with deionized water and stored at -20°C.

Quantitative real-time RT-PCR. After total RNA extraction of the infected cell cultures with TRIZOL Reagent as described previously at 2, 4, 6, 10, and 24 hpi, quantitative real-time reverse transcriptase polymerase chain reaction (RT-PCR) was performed on the samples using primers specific for the 5'-UTR of the BVDV genome. PCR reactions were performed in a final volume of 25 µL with 1.0 µg total RNA as templates used for all samples. The reactions consisted of 14.7 µL master mix containing 2× RT-PCR buffer, 25× BVD Primer probe mix, and 25× RT enzyme mix. Following the reverse transcription step at 45°C for 10 minutes and the initial PCR activation step at 95°C for 10 minutes, the reactions were cycled 40 times with denaturation at 95°C for 15 seconds and annealing at 60°C for 45 seconds in a thermal cycler (Applied Biosystems). CT values generated were compared to a standard curve from a known amount of DNA to determine the RNA copy number.

Semi-quantitative RT-PCR. Total RNA was extracted from samples as described above and semi-quantitative RT-PCR was performed using the OneStep RT-PCR Kit (QIAGEN) in accordance with manufacturer's instruction with 1.0 µg total RNA as templates. Primers specific for 18S rRNA were used as an internal control and Primers BVDVF373 and BVDVR373 were specific for the 5'-UTR of the BVDV genome. The reverse transcription step was carried out in a volume of 50 µL for 30 minutes at 50°C followed by an initial PCR activation step for 15 minutes at 95°C. Reactions were cycled 35 times at 94°C for 45 seconds, 60°C for 45 seconds, 72°C for one minute, and then fi-

nally extended once at 72°C for 5 minutes in a DNA thermal cycler (Eppendorf). Ten microliter aliquots of the RT-PCR products were separated on a 1.2% agarose gel in Tris-acetate-EDTA buffer (40 mM Tris-HCl [pH 7.4], 40 mM acetic acid, 1 mM EDTA) and then visualized with UV illumination after staining with 1.0 μg/mL ethidium bromide.

Statistical analysis. All statistical analyses were performed using the personal computer program GraphPad Prism, version 5.00, for Windows (GraphPad Software, San Diego, California). Antiviral assay results were analyzed by two-way ANOVA with Bonferroni post test. A $p<0.05$ was considered to be statistically significant.

Table 2. Thermal cycler conditions for quantitative real-time RT-PCR.

Stage	Cycles	Temperature (°C)	Time
Reverse transcription	1	45.0	10:00
Initial PCR activation		95.0	10:00
2-step cycling a) Denaturation	40	95.0	0:15
b) Annealing		60.0	0:45

Table 3. Thermal cycler conditions for semi-quantitative RT-PCR.

Stage	Cycles	Temperature (°C)	Time
Reverse transcription		50.0	30:00
Initial PCR activation		95.0	15:00
3-step cycling a) Denaturation	35	94.0	0:45
b) Annealing		55.0	0:45
c) Extension		72.0	1:00
Final extension		72.0	10:00

3. Results

3.1 Toxicity of PPMO in bovine tracheal cell lines

A PMO without the peptide conjugated to the 5' end creates an overall neutral charge for the compound, and so it is not toxic to target cells. However, because the antisense agent needs to be able to enter target cells efficiently, an arginine-rich peptide is covalently conjugated to the 5' end, creating a positively charged PPMO. As a result, having a charged compound can render it toxic if high amounts are present in mammalian cell lines. Thus, a cell toxicity assay was conducted to determine an appropriate PPMO concentration and pre-treatment time for this study. To investigate PPMO cytotoxicity on cell viability, non-infected BT cells were treated with a PPMO that is not sequence-specific for bovine DNA sequences. Drug toxicity was detected by cell degeneration using standard microscopy. Table 2 shows viability results from cells treated with PPMO over a concentration range from 5 to 80 μM for different time periods. Figure 9 are the viability results in the form of a graph showing PPMO treatment after the first (Panel A) and fifth day (Panel B). Results were compared to a control group mock-treated with plain DMEM medium (data not shown).

At the first day of incubation, no significant difference was apparent in viability between mock-treated cells and cells treated with 40 μM of PPMO. However, treatment with 80 μM of PPMO caused cell degeneration by the first day of drug incubation. Treatment of cells for 24 hours at 40 μM and higher caused degeneration, while treatment for 24 hours at 20 μM and lower caused unhealthy morphology compared with the control. At the fifth day of incubation, cells subjected to PPMO treatment for 24 hours were

damaged regardless of drug concentration. In addition, cells pre-treated for 4 hours at 40 μM and higher were not healthy. Thus, PPMO pre-treatment of BT cell lines for 2 hours at 20 μM or less was used for the remainder of the cell culture experiments in this study.

Table 4. Cell toxicity assay data.

Day 1				Day 5		
Condition of Cells				Condition of Cells		
PPMO Concentra-tion (μM)	Treatment Time (hrs) 2	4	24	Treatment Time (hrs) 2	4	24
5	Healthy	Healthy	Unhealthy	Healthy	Healthy	Degeneration
10	Healthy	Healthy	Unhealthy	Healthy	Healthy	Degeneration
20	Healthy	Healthy	Unhealthy	Healthy	Healthy	Degeneration
40	Healthy	Healthy	Degeneration	Healthy	Unhealthy	Degeneration
60	Healthy	Healthy	Degeneration	Unhealthy	Unhealthy	Degeneration
80	Degeneration	Degeneration	Degeneration	Degeneration	Degeneration	Degeneration

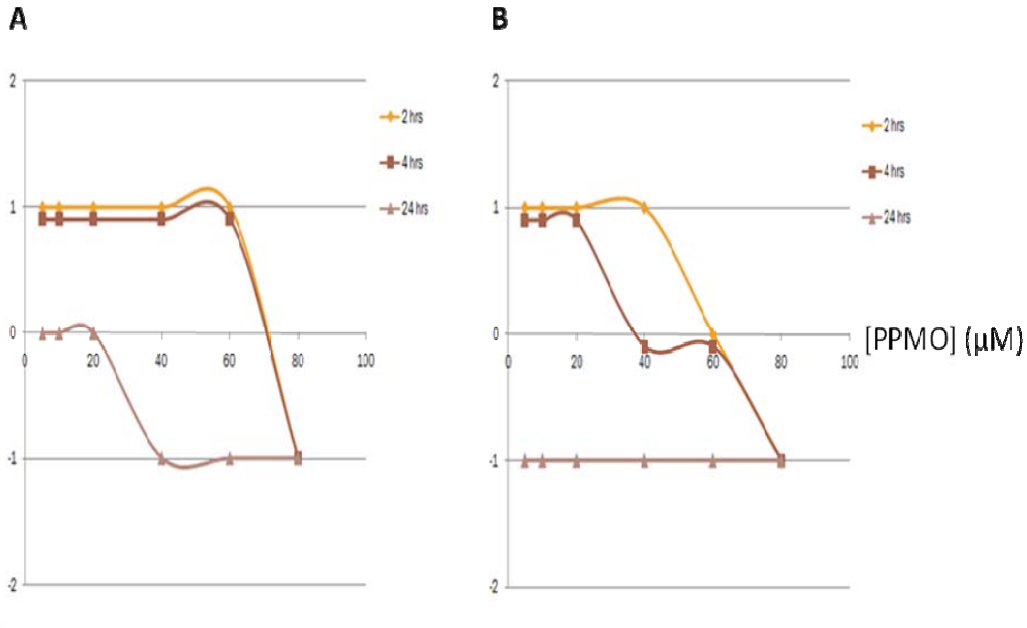

Figure 9. Bovine tracheal cell toxicity analysis. Twelve-well plates were seeded with 1×10^6 BT cells/well the day before PPMO treatment, washed once with 1× DPBS, and were treated with 0.5 mL of a generic PPMO non-specific for bovine DNA sequences at 5, 10, 20, 40, 60, and 80 µM, respectively. At 2, 4, and 24 hours post-treatment, the drug was removed and cells were washed twice with 1× DPBS. DMEM media supplemented with 5% FBS was added, and cell viability was examined using standard microscopy over a period of five days. X-axis is the PPMO concentration, and Y-axis is the condition of the cells after Day 1 (A) and Day 5 (B) of PPMO treatment. Cellular viability was designated a number, where 1=healthy, 0=abnormal morphology, and -1=death or cell detachment from wells. Conditions of the cells were compared to a control mock-treated with plain DMEM medium.

3.2 The effect of binding to *cis*-elements on virus replication

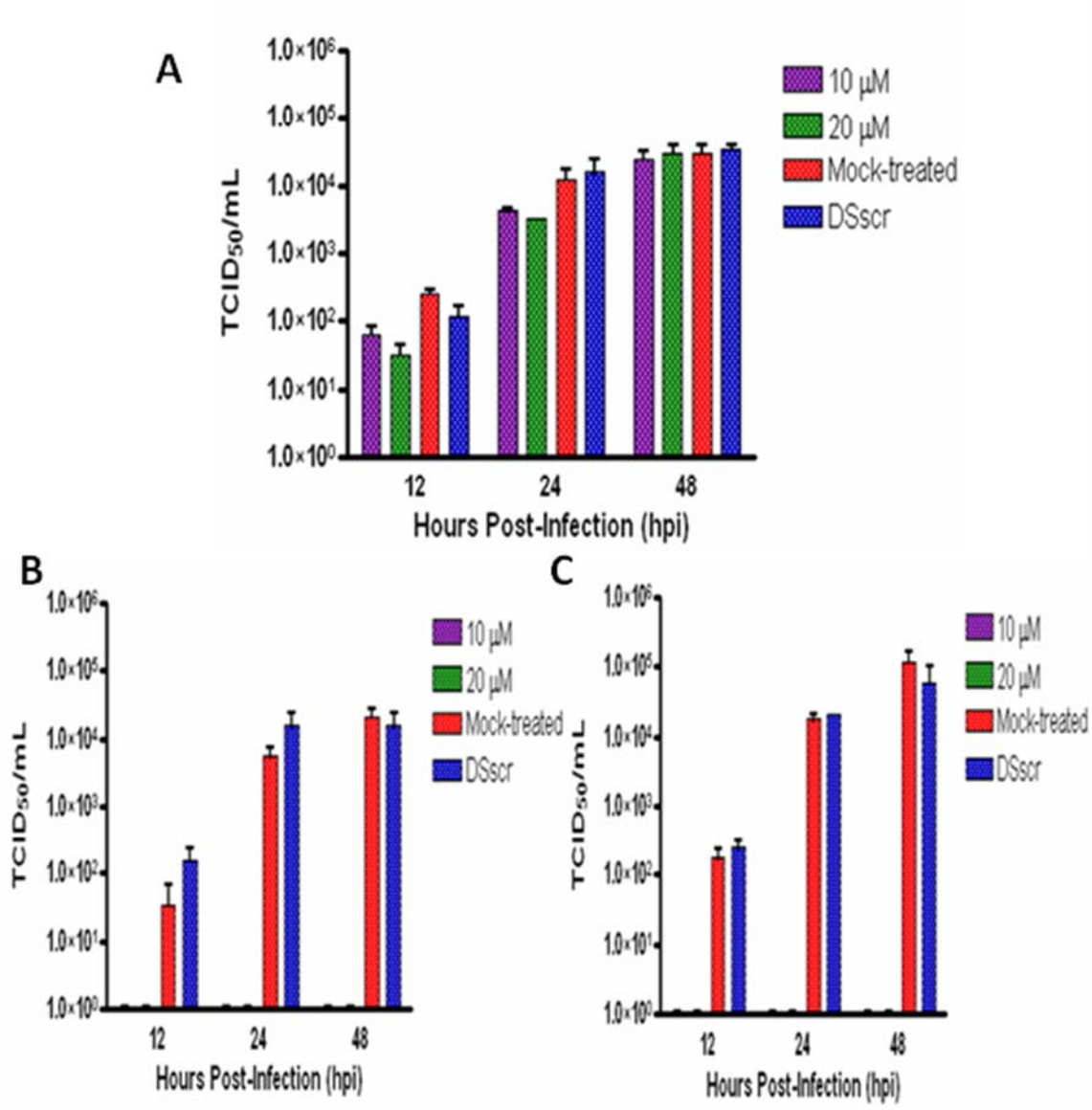

Figure 10. *In vitro* inhibition of BVDV infection with PPMO targeting the 5'-UTR of the BVDV genome. (A) Treatment with PPMO BVDV-10. (B) Treatment with PPMO BVDV-258. (C) Treatment with PPMO BVDV-375. The original virus stock titer for the three treatments was ~10^4 $TCID_{50}$/mL (data not shown). BT cells were pre-treated with the indicated PPMO at indicated concentrations for two hours, and then infected with BVDV (NADL strain) at an MOI of 0.01. Viral yields were determined by the standard $TCID_{50}$ assay as described before (Becher et al., 2001) (n=3).

BVDV growth kinetics following treatment of PPMO BVDV-10

To determine the effect of PPMO targeting nt 10-33 in the 5'-UTR, BT cells were pre-treated with BVDV-10 for 2 hours before BVDV infection, and virus growth was measured at 12, 24, and 48 hpi. As shown in Fig. 10A, DSscr- and mock-treatments had no effect on BVDV growth. The titer differences between mock- and DSscr-treated cells was not statistically significant ($p>0.05$) and DSscr thus had no effect on BVDV replication. Cells pre-treated with 10 μM and 20 μM of PPMO BVDV-10 show about a 5-fold decrease in virus titer compared to DSscr- and mock-treated cells at 12 hpi. The inhibition decreased at 24 hpi and became unapparent at 48 hpi as seen by the lack of titer differences at the 48-hour time point. Statistical analyses, however, show that the titer difference between 10 μM PPMO BVDV-10 with mock and DSscr treatment at all time points was not statistically significant ($p>0.05$). Titer differences between 20 μM PPMO BVDV-10 with mock and DSscr treatment at the three time points was also not statistically significant ($p>0.05$). In addition, titer differences between the two concentrations of PPMO BVDV-10 at the three time points was not statistically significant ($p>0.05$). Thus, although PPMO BVDV-10 appears to demonstrate some initial inhibition between 12 and 24 hpi, the titer differences between the drug-treated and untreated groups were not statistically significant.

BVDV growth kinetics following treatment of PPMO BVDV-258 and BVDV-375

To determine the effect of PPMO targeting nt 258-281 in the 5'-UTR, BT cells were pre-treated with BVDV-258 for 2 hours before BVDV infection, and virus growth was measured at 12, 24, and 48 hpi as described previously with BVDV-10 treatment. As shown in Fig. 10B, PPMO treatment showed complete inhibition of BVDV replication at all three time points. The random sequence DSscr had no observable effect on BVDV replication as DSscr-treated cells produced nearly identical results to mock-treated. The lack of virus titer with the PPMO-treated compared to the mock- and DSscr-treated cells demonstrates that the PPMO produced an inhibition effect on virus replication.

Similar to PPMO BVDV-258, BT cells were pre-treated with PPMO BVDV-375 to determine the importance of the AUG initiation codon by targeting nt 375-398 of the 5'-UTR. Again, results (Fig. 10C) demonstrate complete inhibition of BVDV replication at all three time points, and the DSscr had no observable effects on BVDV replication as both controls produced nearly identical results. Thus, both BVDV-258 and BVDV-375 were able to completely inhibit viral replication.

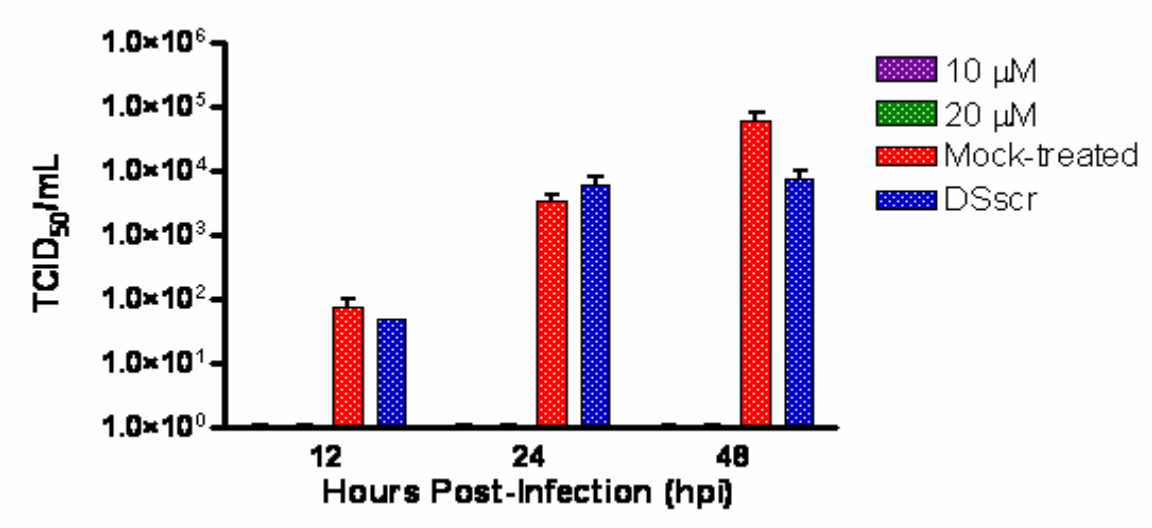

Figure 11. *In vitro* inhibition of BVDV infection with PPMO BVDV-12503 targeting the 3'-UTR of the BVDV genome. The procedure was identical to treatment with PPMO targeting the 5'-UTR (see Figure 10). The original virus stock titer for the treatment was ~10^4 $TCID_{50}$/mL (data not shown).

BVDV growth kinetics following treatment of PPMO BVDV-12503

PPMO BVDV-12503 was used to target nt 12503-12526 of the 3'-UTR to determine the importance of the conserved SS region. BT cells pre-treated with 10 µM and 20 µM of PPMO BVDV-12503 showed complete inhibition of BVDV replication at all three time points (Figure 11). As with the previous drug treatments, the random sequence DSscr had no observable effects on BVDV replication as DSscr-treated cells produced nearly identical results to mock-treated. The lack of virus titer with PPMO BVDV-12503-treated cells compared to the mock- and DSscr-treated cells demonstrate that this 3'-UTR PPMO was able to produce an inhibition effect similar to BVDV-258 and BVDV-375.

3.3 The effects on viral genome replication

Generation of DNA standard for quantitative real-time RT-PCR

In order to measure the viral genome copy number by quantitative real-time RT-PCR, a portion of the 5'-UTR was amplified by RT-PCR and the product was cloned into a pCR2 TOPO cloning vector. Correct insertion was verified by restriction enzyme digestion with EcoRI. As shown in Figure 12, the top bands in lanes 1 and 2 represent the vector (~3900 bp). The smaller bands at 225 bp in lanes 1 and 2 represent the BVDV insert. The purified plasmid was used to establish the standard curve for quantitative real-time RT-PCR.

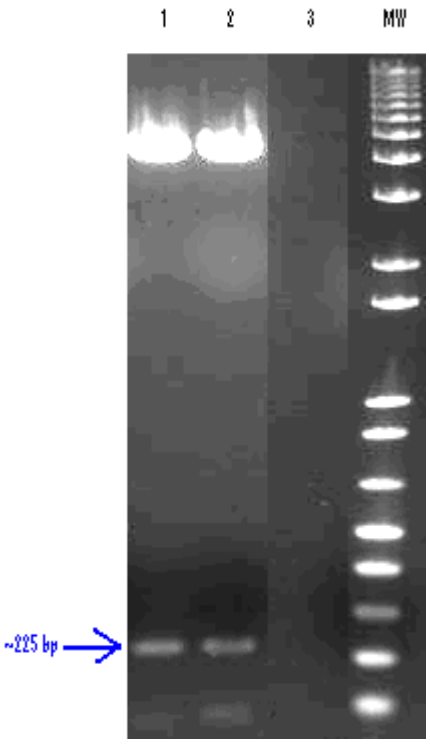

Figure 12. Detection of the BVDV insert by restriction enzyme digestion and gel electrophoresis. Lanes 1 & 2: TOPO cloning vector (top band) and the 5'-UTR BVDV insert (bottom band); 3: negative control; MW: 1 Kb Plus DNA Ladder (1.0 µg/µL) (Invitro-

gen). Chemically competent *E. coli* cells were transformed with a pCR2 TOPO vector ligated to part of the BVDV 5'-UTR sequence. After purification of the plasmid, restriction enzyme digestion was performed with EcoRI, and the two fragments were separated out on a 1.2% agarose gel. Serial dilutions of the plasmid were made before being subjected to quantitative real-time PCR.

Serial dilutions of the BVDV plasmid were made to generate a standard curve to determine the RNA copy number from the drug-treated and untreated samples. The standard curve is shown below, where an increase of 3 cycle threshold (CT) value units correlates to an approximate 10-fold decrease in RNA copy number.

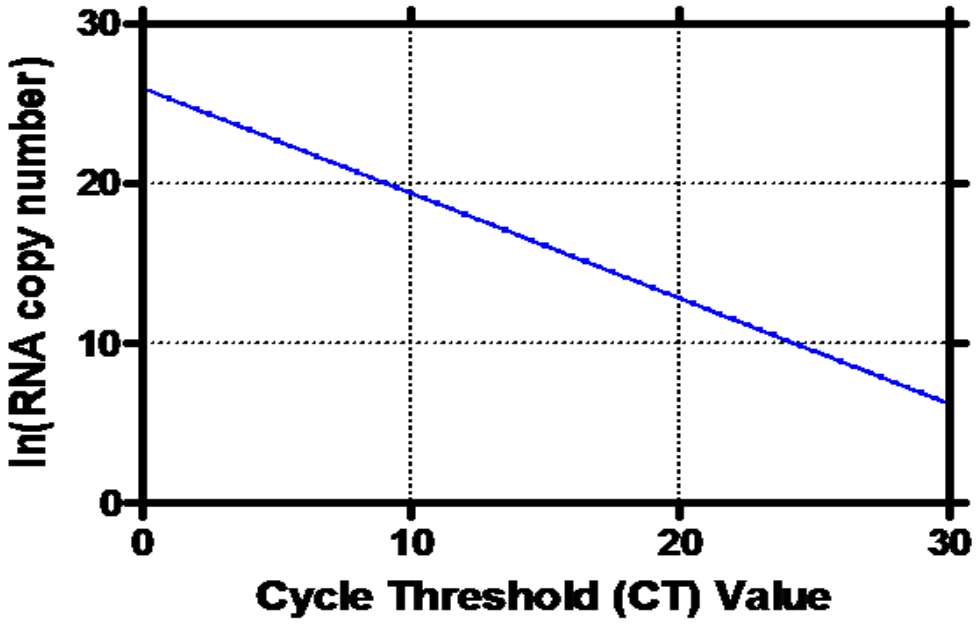

Figure 13. Standard curve for determining RNA copy number from BVDV clone. X-axis is the CT value from quantitative real-time RT-PCR, and Y-axis is the natural logarithm of the RNA copy number.

PPMO BVDV-375 treatment effect on viral RNA synthesis

Since PPMO BVDV-375 completely inhibited virus growth, its effect on viral genome replication was examined by quantitative real-time RT-PCR at 2, 4, 6, 10, and 24 hpi. BT cells were pre-treated with BVDV-375 for two hours before BVDV infection, and then total RNA was extracted at the indicated time points. The extracted RNA was reverse transcribed to cDNA, and then the RT-PCR product was amplified and quantified at the end of each cycle. As shown in Fig. 14, there are little differences in RNA copy number between the two drug-treated groups and the mock-treated group at 2 and 4 hpi. The RNA copy number increases from 2 to 4 hpi and then decreases after 4 hpi in all groups, which is indicative of the lack of RNA-dependent RNA polymerase to synthesize RNA. However, in the drug-treated cells, RNA synthesis is insignificant and remains at a constant low after 10 hpi, while there is a gradual increase in RNA synthesis in mock-treated cells starting shortly before 6 hpi. The 1 log difference at 10 hpi between drug-treated and mock-treated and 2 log difference at 24 hpi demonstrates that PPMO BVDV-375 was able to inhibit BVDV replication at the RNA synthesis level due to the decrease of RNA copy number in both drug-treated groups starting at 6 hpi.

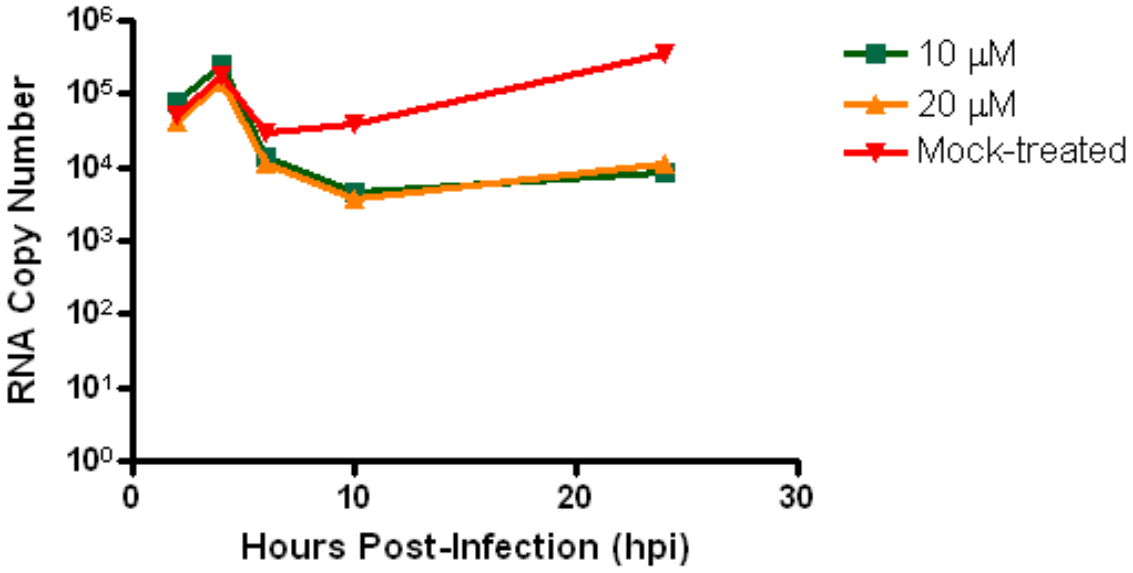

Figure 14. Quantitative real-time RT-PCR analysis of PPMO activity. BT cell cultures were pre-treated with 10 µM PPMO BVDV-375, 20 µM PPMO BVDV-375, or plain DMEM (mock treatment) for two hours, and then infected with BVDV (NADL strain) at an MOI of 0.01. At the indicated times post-infection, cell cultures were harvested, total RNA was extracted with TRIZOL (Invitrogen), and 1.0 µg of RNA template was subjected to quantitative real-time RT-PCR. The CT values obtained were converted to RNA copy number values (n=3).

PPMO BVDV-375 and BVDV-12503 treatment Effect on viral RNA synthesis

Both PPMO BVDV-375 and BVDV-12503 completely inhibited virus growth, and thus their effect at the viral genome replication level was examined by using semi-quantitative RT-PCR at 0, 2, 4, 6, 8, 10, 12, 24, and 48 hpi. Another reason for choosing the two PPMO was to examine differing degrees, if there are any, of viral RNA synthesis inhibition between treatment with BVDV-375, a PPMO that targets the 5'-UTR, and BVDV-12503, a PPMO that targets the 3'-UTR. Quantitative real-time RT-PCR coupled with semi-quantitative RT-PCR can provide an accurate means of detecting trends of

RNA levels and to further confirm the RNA synthesis inhibition with BVDV-375. BT cells were pre-treated with BVDV-375 or BVDV-12503 for two hours before BVDV infection, and then total RNA was extracted at different times post-infection. The extracted RNA was reverse-transcribed and the RT-PCR product was amplified using primers specific for the 5'-UTR of the BVDV genome or 18S rRNA, which serves as the internal control. As shown in Fig. 15, both the drug-treated groups showed either little or lack of RT-PCR product using primers specific for the 5'-UTR (Figure 15A). The mock- and DSscr-treated groups both showed nearly identical patterns of increasing RT-PCR product band intensity, demonstrating that the random sequence DSscr had no effect on BVDV replication. The size of the amplified region was about 373 bp. Panel B shows RT-PCR product amplification of all groups using primers specific for 18S rRNA, demonstrating that cell cultures in both drug- and untreated were similar and that inhibition effects were not due to some other variable in the cell cultures. Thus, both PPMO BVDV-375 and BVDV-12503 were able to inhibit BVDV replication at the RNA synthesis level.

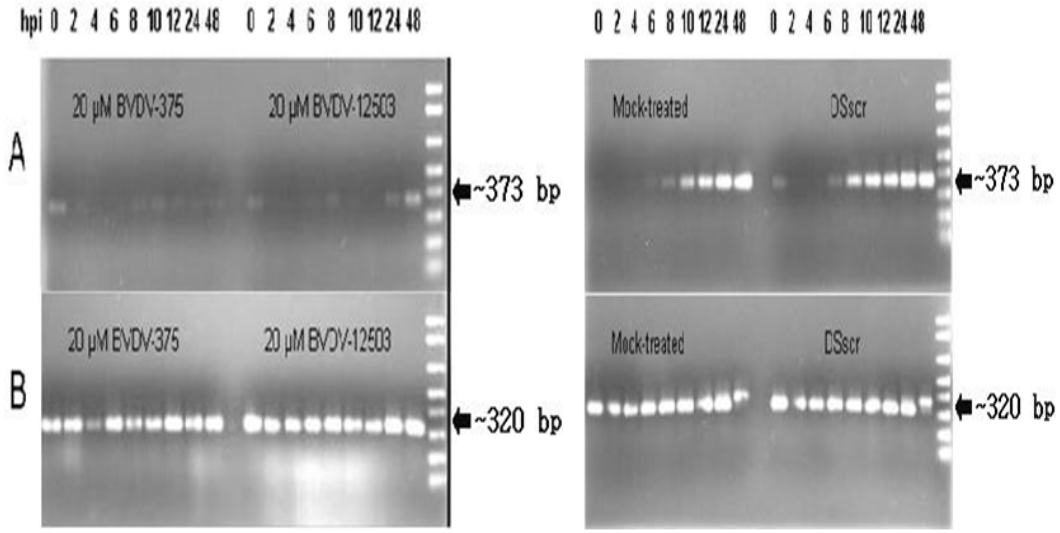

Figure 15. Semi-quantitative RT-PCR analysis of PPMO activity. BT cells were pre-treated with 20 µM PPMO BVDV-375, 20 µM PPMO BVDV-12503, plain DMEM (mock treatment), or 20 µM DSscr for two hours, and then infected with BVDV (NADL strain) at an MOI of 0.01. At the indicated times post-infection, cell cultures were harvested, total RNA was extracted, and 1.0 µg of total RNA template was reverse transcribed using the OneStep RT-PCR Kit (QIAGEN) and PCR amplified with primers specific for the 5'-UTR of the BVDV genome (A) and cellular 18S rRNA (B). The 18S rRNA was used as an internal control.

4. Discussion

The experimental results described here demonstrate that PPMO targeting sequences in the 5'- and 3'-UTR can interfere with BVDV viral replication and viral genome replication *in vitro*. Each evaluation of antiviral efficacy by PPMO in this study included efforts to control for non-sequence-specific effects by including a negative control PPMO, DSscr, in the experiments. Cell viability assays performed on non-infected cells showed little or no cytotoxic effects by the PPMO at up to concentrations of 20 μM and pre-treatment time of 2 hours, under the same cell culture conditions in which the PPMO demonstrated high antiviral activity.

The lack of inhibition of viral activity with BVDV-10 supports some previous studies involving pestivirus IRESes. The BVDV IRES is suggested to start within Domain II and extend into the actual ORF, whereas the target specificity of BVDV-10 occurs outside of the IRES. This is suggestive that the 5' end of the 5'-UTR may not be essential for virus replication. Instead, the region may possess minor roles in secondary structural maintenance of other more important regions that may contain signals for replication. However, there is also differing ideas in recent publications regarding the importance of Domain I. For example, the 5' terminal of the BVDV 5'-UTR has been speculated to contain the signal for RNA replication (Martínez-Salas et al., 2008). Other studies have also mentioned its importance as a bifunctional motif by enhancing gene expression in addition to serving as a replication signal for RNA (Grassmann et al., 2005). Nonetheless, our study demonstrated that even when BVDV-10 was used to create a steric block at the 5' end, virus replication was still observed. Thus, it is possible that other RNA replica-

tion signals exist in the 5'- or 3'-UTR, which suggests that nt 10-33 in the 5'-UTR does not contain secondary structures critical for 5'-UTR function. Another issue regarding the targeted *cis*-sequence of BVDV-10 is the possibility that the PPMO was not able to anneal to its target properly. The PPMO may not have been able to find its target, and even if annealing did take place partial hybridization may have occurred instead, which prevented inhibition of virus replication if Domain I is indeed essential for BVDV replication. Further studies using site-directed mutagenesis could be used to examine the importance of Domain I.

Binding PPMO BVDV-258 and BVDV-375 to targeted sequences may interfere with the secondary structure of the 5'-UTR or the IRES within the 5'-UTR. BVDV-258 targeted a mostly conserved region in Domain III, which is part of proposed pestivirus IRESes mentioned in recent publications such as Grassmann et al., 2005. It is possible that PPMO BVDV-258 prohibits host factors to bind to the IRES and inhibit virus replication. BVDV-375 targeted most of Domain IV and created a steric block over the AUG start codon. The lack of virus replication in cells treated with BVDV-375 suggests that nt 375-398, which includes the AUG initiation codon, is important for translation initiation.

The targeted sequence of PPMO BVDV-12503 at the 3'-UTR is highly conserved in different strains of BVDV, and is suggested to have an important function during virus replication. PPMO binding to these sequences resulted in a decrease in virus replication and RNA replication, which suggests that this *cis*-sequence at the 3'-UTR is important for BVDV replication. Identification of these important elements will allow us to dissect out its specific function during the entire virus replication cycle by point or deletion mu-

tations. In addition, it has been proposed, along with the 3' terminal C residue stretch and SL I, to function as an RNA element responsible for directly facilitating the initiation of negative-sense RNA synthesis. Both the 3' terminal C residue stretch and SL I have also been shown to be indispensable for virus replication.

Quantitative real-time RT-PCR was used to measure the RNA copy number of both mock-treated and drug-treated cell cultures at different times post-infection. PPMO BVDV-375 was demonstrated earlier to be able to completely inhibit virus replication and thus was used in this experiment. Treatment with negative controls was done for mock-treatment only due to the similar virus titers shown from the antiviral assays earlier between mock- and DSscr-treated. Thus, for economical and redundancy reasons, treatment with DSscr was omitted in this analysis.

The changes in RNA copy number over time as deduced from quantitative real-time RT-PCR can be used to roughly illustrate the BVDV infection cycle. Following the initial phase with the adsorption of BVDV, the eclipse phase begins. In this stage, there is no synthesis of new virions until genome replication begins. Input virus becomes uncoated, meaning that no infectious virus can be detected during this period. The capsid breaks down to release the viral genome, which is most probable during 2 to 6 hpi where the RNA copy number gradually decreases. Then, the virus enters the synthetic phase, in which new viral particles are assembled by positive-sense RNA synthesis and protein production. Starting shortly before 6 hpi into the infection cycle is most likely when the synthetic phase begins, as seen with the gradual increase of RNA copy number. At this time, more RNA-dependent RNA polymerase proteins are made, and more RNA mole-

cules are replicated and produced. This matches the published data by Gong et al., 1996, where northern blot hybridization was used to look at RNA synthesis at different times post-infection. In this study, the authors showed that positive-sense RNA synthesis increased starting at 6 hpi, which corresponds to our results in Figure 14. Compared to the mock-treated cells, both drug-treated cells did not experience increases in RNA copy number at 6 hpi, suggesting inhibition at the RNA replication level. Both 10 and 20 μM of PPMO BVDV-375 inhibited RNA synthesis during the synthetic phase, and thus the increase of PPMO concentration from 10 to 20 μM did not result in a significant difference since both concentrations produced similar RNA copy number values at each time point.

The data demonstrates that pre-treatment of cells with PPMO BVDV-375 results in a decrease in viral RNA copy number. Though RNA synthesis decreases until 10 hpi in the PPMO-treated cells, RNA levels do not drop below 10^3 copies. In addition, RNA synthesis seems to increase slightly at the 24 hpi time point compared to 10 hpi. A possible explanation could be the limited effect PPMO has on *cis*-sequence binding. The antisense compound finds its target and binds to the UTR but may eventually lose binding ability over time. Nonetheless, because there is a difference of RNA copy numbers between the untreated and treated groups, the data shows that the AUG start codon and the stretch of nucleotides before the triplet in Domain IV not only have roles in translation initiation, but may also be important for RNA replication. An alternative way of explaining the decrease in RNA copy number is that the blocking of translation initiation hinders the synthesis of RNA if signals for both processes are dependent on each other. As a result, all

the functional elements cease to function if one of them is inhibited, which is especially true if there were no other means of initiating translation. Experiments involving RNA-protein interactions and site-directed mutagenesis would need to be conducted to determine functions of each functional element in the 5'-UTR and whether these RNA elements possess more than one role.

Another interesting observation is that result comparisons of the *in vitro* inhibition and quantitative real-time RT-PCR analysis of PPMO BVDV-375 revealed an approximate four-fold difference of virus titer yet only a two-fold difference of RNA copy number between the PPMO- and non-treated, respectively. A possible explanation is that even though there was some RNA synthesis inhibition, protein translation was still able to occur, leading to the production of more virions and thus a higher virus titer. Further studies with protein immunoblots using antibodies specific for the E2 glycoprotein may provide some insight on the discrepancy of virus titer and RNA copy number at the same hpi. Another explanation is again with the partial hybridization of the PPMO, where RNA copy numbers would have been higher in the quantitative real-time RT-PCR analysis if the PPMO remained fully hybridized to its target *cis*-sequence.

Semi-quantitative RT-PCR was also used to examine PPMO antiviral activity at the viral genome level. The treated and untreated groups were subjected to reverse transcription using primers specific for 18S rRNA or the 5'-UTR of the BVDV genome, where primers specific for 18S rRNA were used as an internal control. Levels of cellular 18S rRNA transcript were constant through time for both PPMO and mock-treated cells, indicating that the treatments did not have off-target effects. Even though the amplified 18S

rRNA product was supposed to be 488 bp, the actual size in the gel was about 160 bp less (see Figure 15B). The unexpected size difference is not significant since amplified product was present at all time points in both groups. To further investigate the unexpected size difference, however, a different set of primers can be used to amplify the 18S rRNA product before subjecting the product to sequencing.

The little or lack of RT-PCR product in the drug-treated groups compared to the mock- and DSscr-treated demonstrates that inhibition by PPMO BVDV-375 and BVDV-12503 is present at the RNA synthesis level. This suggests that the regions targeted by both PPMO are important for RNA replication since the steric block prevented synthesis of RNA. Again, inhibition at the RNA replication level was already demonstrated with PPMO BVDV-375 earlier with quantitative real-time RT-PCR. Results with semi-quantitative RT-PCR further support it. The demonstration of RNA replication inhibition with PPMO BVDV-12503 provides more support of two important ideas mentioned in the literature regarding the highly conserved targeted sequence: (1) the nucleotide sequence is conserved among five BVDV strains and thus suggests an essential role for virus replication, and (2) the stretch of C residues at the 3' end, SS, and SL I make up a functional element responsible for synthesizing negative-sense RNA.

5. Conclusion

In this study, antisense compounds similar to DNA called PPMO were used to study the replication mechanism of BVDV, an animal pathogen known to cause infections in cattle. Virus replication was supported in bovine tracheal (BT) cell lines. A cell toxicity assay using standard microscopy demonstrated that PPMO concentrations of 20 μM or less with a pre-treatment time of less than four hours were not cytotoxic to BT cells, while higher concentrations and longer pre-treatment times eventually caused cell degeneration. At both concentrations of 10 μM and 20 μM, two PPMO that target the 5'-UTR of the BVDV genome, BVDV-258 and BVDV-375, were able to completely inhibit BVDV replication, while PPMO BVDV-10 did not completely block virus replication. In addition, the 3'-UTR PPMO BVDV-12503 was also able to completely inhibit virus replication. Analysis of PPMO BVDV-375 antiviral activity with quantitative real-time RT-PCR demonstrated decreases in the viral RNA copy number starting shortly before 6 hpi, while the copy number in mock-treated cells gradually increased around 6 hpi. Analysis of PPMO BVDV-375 and BVDV-12503 antiviral activity with semi-quantitative RT-PCR showed a decrease in amplified RT-PCR product from extracted RNA compared to mock- and DSscr-treated. These results demonstrate that the PPMO inhibited BVDV replication at the RNA synthesis level and that the targeted regions in both the 5'- and 3'-UTR have important roles in virus replication.

Future work on this project, if possible, can include further studies on specific regions of both the 5'- and 3'-UTR of the BVDV genome, especially their roles in initiating translation. Previous studies have mentioned the IRES having a major role in initiating

translation independent of a 5' cap structure, which can include recruitment of ribosomal complexes and serving as a ribosome landing pad. Thus, the next step would be to determine the exact boundaries of the IRES, including the controversial 5' boundary and where it ends in the coding region of the ORF. Also, because PPMO BVDV-12503 targets the 3'-UTR and was able to inhibit virus replication, further studies on the 3'-UTR can provide insight on the specific functions of each RNA element and what role each component has in BVDV replication.

REFERENCES

Becher, P., Orlich, M., and H.J. Thiel. 2001. RNA recombination between persisting pestivirus and a vaccine strain: Generation of cytopathogenic virus and induction of lethal disease. *Journal of Virology* 75:6256-6264.

Bok, K., Cavanaugh, V.J., Matson, D.O., González-Molleda, L., Chang, K.O., Zintz, C., Smith, A.W., Iversen, P., Green, K.Y., and A.E. Campbell. 2008. Inhibition of norovirus replication by morpholino oligomers targeting the 5'-end of the genome. *Virology* 380:328-337.

Booker, C.W., Abutarbush, S.M., Morley, P.S., Guichon, P.T., Wildman, B.K., Jim, G.K., Schunicht, O.C., Pittman, T.J., Perrett, T., Ellis, J.A., Appleyard, G., and D.M. Haines. 2008. The effect of bovine viral diarrhea virus infections on health and performance of feedlot cattle. *The Canadian Veterinarian Journal* 49:253-260.

Brown, E.A., Zhang, H., Ping, L., and S.M. Lemon. 1992. Secondary structure of the 5' nontranslated regions of hepatitis C virus and pestivirus genomic RNAs. *Nucleic Acids Research* 20:5041-5045.

Burrer, R., Neuman, B.W., Ting, J.P.C., Stein, D.A., Moulton, H.M., Iversen, P.L., Kuhn, P., and M.J. Buchmeier. 2007. Antiviral effects of antisense morpholino oligomers in murine coronavirus infection models. *Journal of Virology* 81:5637-5648.

Chon, S.K., Perez, D.R., and R.O. Donis. 1998. Genetic analysis of the internal ribosome entry segment of bovine viral diarrhea virus. *Virology* 251:370-382.

Deas, T.S., Binduga-Gajewska, I., Tilgner, M., Ren, P., Stein, D.A., Moulton, H.M., Iversen, P.L., Kauffman, E.B., Kramer, L.D., and P.Y. Shi. 2005. Inhibition of flavivirus infections by antisense oligomers specifically suppressing viral translation and RNA replication. *Journal of Virology* 79:4599-4609.

Deng, R., and K.V. Brock. 1993. 5' and 3' untranslated regions of pestivirus genome: primary and secondary structure analyses. *Nucleic Acids Research* 21:1949-1957.

Fletcher, S.P., and R.J. Jackson. 2002. Pestivirus internal ribosome entry site (IRES) structure and functions: Elements in the 5' untranslated region important for IRES function. *Journal of Virology* 76:5024-5033.

Fulton, R.W., Briggs, R.E., Ridpath, J.F., Saliki, J.T., Confer, A.W., Payton, M.E., Duff, G.C., Step, D.L., and D.A. Walker. 2005. Transmission of bovine viral diarrhea virus 1b to susceptible and vaccinated calves by exposure to persistently infected calves. *Canadian Journal of Veterinary Research* 69:161-169.

Fulton, R.W., Ridpath, J.F., Ore, S., Confer, A.W., Saliki, J.T., Burge, L.J., and M.E. Payton. 2005. Bovine viral diarrhea virus (BVDV) subgenotypes in diagnostic laboratory accessions: Distribution of BVDV1a, 1b, and 2a subgenotypes. *Veterinary Microbiology* 111:35-40.

Gabriel, G., Nordmann, A., Stein, D.A., Iversen, P.L., and H.D. Klenk. 2008. Morpholino oligomers targeting the PB1 and NP genes enhance the survival of mice infected with highly pathogenic influenza A H7N7 virus. *Journal of General Virology* 89:939-948.

Gamarnik, A.V., and R. Andino. 1998. Switch from translation to RNA replication in a positive-strand RNA virus. *Genes & Development* 12:2293-2304.

Ge, Q., Pastey, M., Kobasa, D., Puthavathana, P., Lupfer, C., Bestwick, R.K., Iversen, P.L., Chen, J., and D.A. Stein. 2006. Inhibition of multiple subtypes of influence A virus in cell cultures with morpholino oligomers. *Antimicrobial Agents and Chemotherapy* 50:3724-3733.

Gong, Y., Trowbridge, R., Macnaughton, T.B., Westaway, E.G., Shannon, A.D., and E.J. Gowans. 1996. Characterization of RNA synthesis during a one-step growth curve and of the replication mechanism of bovine viral diarrhea virus. *Journal of General Virology* 77:2729-2736.

Grassman, C.W., Yu, H., Isken, O., and S.E. Behrens. 2005. Hepatitis C virus and the related bovine viral diarrhea virus considerably differ in the functional organization of the 5' non-translated region: Implications for the viral life cycle. *Virology* 333: 349-366.

Han, X., Fan, S., Patel, D., and Y.J. Zhang. 2009. Enhanced inhibition of porcine reproductive and respiratory syndrome virus replication by combination of morpholino oligomers. *Antiviral Research* 82:59-66.

Isken, O., Baroth, M., Grassman, C.W., Weinlich, S., Ostareck, D.H., Ostareck-Lederer, A., and S.E. Behrens. 2007. Nuclear factors are involved in hepatitis C virus RNA replication. *RNA* 13:1675-1692.

Isken, O., Grassman, C.W., Sarisky, R.T., Kann, M., Zhang S., Grosse, F., Kao, P.N., and S.E. Behrens. 2003. Members of the NF90/NFAR protein group are involved in the life cycle of a positive-strand RNA virus. *The EMBO Journal* 22:5655-5665.

Isken, O., Grassmann, C.W., Yu, H., and S.E. Behrens. 2004. Complex signals in the genomic 3' nontranslated region of bovine viral diarrhea virus coordinate translation and replication of the viral RNA. *RNA* 10:1637-1652.

Ivanyi-Nagy, R., Lavergne, J.P., Gabus, C., Ficheux, D., and J.L. Darlix. 2008. RNA chaperoning and intrinsic disorder in the core proteins of flaviviridae. *Nucleic Acids Research* 36:712-725.

Kolupaeva, V.G., Pestova, T.V., and C.U.T. Hellen. 2000. Ribosomal binding to the internal ribosomal entry site of classical swine fever virus. *RNA* 6:1791-1807.

Lupfer, C., Stein, D.A., Mourich, D.V., Tepper, S.E., Iversen, P.L., and M. Pastey. 2008. Inhibition of influenza A H3N8 virus infections in mice by morpholino oligomers. *Archives of Virology* 153:929-937.

Martínez-Salas, E., Pacheco, A., Serrano, P., and N. Fernandez. 2008. New insights into internal ribosome entry site elements relevant for viral gene expression. *Journal of General Virology* 89:611-626.

Moes, L., and M. Wirth. 2007. The internal initiation of translation in bovine viral diarrhea virus RNA depends on the presence of an RNA pseudoknot upstream of the initiation codon. *Journal of Virology* 4:124.

Moulton, H.M., Nelson, M.H., Hatlevig, S.A., Reddy, M.T., and P.L. Iversen. 2004. Cellular uptake of antisense morpholino oligomers conjugated to arginine-rich peptides. *Bioconjugate Chemistry* 15:290-299.

Murray, C.L., Marcotrigiano, J., and C.M. Rice. 2008. Bovine viral diarrhea virus core is an intrinsically disordered proteins that binds RNA. *Journal of Virology* 82:1294-1304.

Neuman, B.W., Stein, D.A., Kroeker, A.D., Churchill, M.J., Kim, A.M., Kuhn, P., Dawson, P., Moulton, H.M., Bestwick, R.K., Iversen, P.L., and M.J. Buchmeier. 2005. Inhibition, escape, and attenuated growth of severe acute respiratory syndrome coronavirus treated with antisense morpholino oligomers. *Journal of Virology* 79:9665-9676.

Paeshuyse, J., Leyssen, P., Mabery, E., Boddeker, N., Vrancken, R., Froeyen, M., Ansari, I.H., Dutartre, H., Rozenski, J., Gil, L.H.V.G., Letellier, C., Lanford, R., Canard, B., Koenen, F., Kerkhofs, P., Donis, R.O., Herdewijn, P., Watson, J., Clercq, E.D., Puerstinger, G., and J. Neyts. 2006. A novel, highly selective inhibitor of pestivirus replication that targets the viral RNA-dependent RNA polymerase. *Journal of Virology* 80:149-160.

Paessler, S., Rijnbrand, R., Stein, D.A., Ni, H., Yun, N.E., Dziuba, N., Borisevich, V., Seregin, A., Ma, Y., Blouch, R., Iversen, P.L., and M.A. Zacks. 2008. Inhibition of alphavirus infection in cell culture and in mice with antisense morpholino oligomers. *Virology* 376:357-370.

Pankraz, A., Thiel, H.J., and P. Becher. 2005. Essential and nonessential elements in the 3' nontranslated region of bovine viral diarrhea virus. *Journal of Virology* 79:9119-9127.

Patel, D., Opriessnig, T., Stein, D.A., Halbur, P.G., Meng, X.J., Iversen, P.L., and Y.J. Zhang. 2008. Peptide-conjugated morpholino oligomers inhibit porcine reproductive and respiratory syndrome virus replication. *Antiviral Research* 77:95-107.

Ridpath, J.F., Neill, J.D., Vilcek, S., Dubovi, E.J., and S. Carman. 2006. Multiple outbreaks of severe acute BVDV in North America occurring between 1993 and 1995 linked to the same BVDV2 strain. *Veterinary Microbiology* 114:196-204.

Rijnbrand, R., Thiviyanathan, V., Kaluarachchi, K., Lemon, S.M., and D.G. Gorenstein. 2004. Mutational and structural analysis of stem-loop IIIc of the hepatitis C virus and GB virus B internal ribosome entry sites. *Journal of Molecular Biology* 343:805-817.

Sleeman, K., Stein, D.A., Tamin, A., Reddish, M., Iversen, P.J., and P.A. Rota. 2009. Inhibition of measles virus infections in cell cultures by peptide-conjugated morpholino oligomers. *Virus Research* 140:49-56.

Smith, D.R., and D.M. Grotelueschen. 2004. Biosecurity and biocontainment of bovine viral diarrhea virus. *Vet Clin North Am Food Anim Pract* 20:131-149.

Stein, D.A. 2008. Inhibition of RNA virus infections with peptide-conjugated morpholino oligomers. *Current Pharmaceutical Design* 14:2619-2634.

Stein, D.A., Huang, C.Y., Silengo, S., Amantana, A., Crumley, S., Blouch, R.E., Iversen, P.L., and R.M. Kinney. 2008. Treatment of AG129 mice with antisense morpholino oligomers increases survival time following challenge with dengue 2 virus. The Journal of Antimicrobial Chemotherapy 62:555-565.

Stone, J.K., Rijnbrand, R., Stein, D.A., Ma, Y., Yang, Y., Iversen, P.L., and R. Andino. 2008. A morpholino oligomer targeting highly conserved internal ribosome entry site sequence is able to inhibit multiple species of picornavirus. *Antimicrobial Agents and Chemotherapy* 52:1970-1981.

Summerton, J., and D. Weller. 1997. Morpholino antisense oligomers: design, preparation, and properties. *Antisense Nucleic Acid Drug Dev* 7:187-195.

Thiel, H.J., Plagemann, P.G.W., and V. Moennig. 1996. Pestiviruses. *Fields Virology* 3:1059-1069.

Vagnozzi, A., Stein, D.A., Iversen, P.L., and E. Rieder. 2007. Inhibition of foot-and-mouth disease virus infections in cell cultures with antisense morpholino oligomers. *Journal of Virology* 81:11669-11680.

Yu, H., Grassman, C.W., and S.E. Behrens. 1999. Sequence and structural elements at the 3' terminus of bovine viral diarrhea virus genomic RNA: Functional role during RNA replication. *Journal of Virology* 73:3638-3648.

Yuan, J., Stein, D.A., Lim, T., Qiu, D., Coughlin, S., Liu, Z., Wang, Y., Blouch, R., Moulton, H.M., Iversen, P.L., and D. Yang. 2006. Inhibition of coxsackievirus B3 in cell cultures and in mice by peptide-conjugated morpholino oligomers targeting the internal ribosome entry site. *Journal of Virology* 80:11510-11519.

Zhang, B., Dong, H., Stein, D.A., and P.Y. Shi. 2008. Co-selection of West Nile virus nucleotides that confer resistance to an antisense oligomer while maintaining long-distance RNA/RNA base pairings. *Virology* 382:98-106.

Zhang, G., Aldridge, S., Clarke, M.C., and J.W. McCauley. 1996. Cell death induced by cytopathic bovine viral diarrhea virus is mediated by apoptosis. *Journal of General Virology* 77:1677-1681.

Zhang, Y.J., Wang, K.Y., Stein, D.A., Patel, D., Watkins, R., Moulton, H.M., Iversen, P.L., and D.O. Matson. 2007. Inhibition of replication and transcription activator and latency-associated nuclear antigen of kaposi's sarcoma-associated herpesvirus by morpholino oligomers. *Antiviral Research* 73:12-23.